Soft Matter

TUTORIAL REVIEW

View Article Online
View Journal | View Issue

Cite this: *Soft Matter*, 2025, **21**, 8602

Myxococcus xanthus for active matter studies: a tutorial for its growth and potential applications

Jesus Manuel Antúnez Domínguez, *[a] Laura Pérez García,[a] Natsuko Rivera-Yoshida,[b] Jasmin Di Franco,[cd] David Steiner,[c] Alejandro V. Arzola,[e] Mariana Benítez,[f] Charlotte Hamngren Blomqvist,[a] Roberto Cerbino,[c] Caroline Beck Adiels[a] and Giovanni Volpe *[ag]

Received 19th March 2025,
Accepted 24th October 2025

DOI: 10.1039/d5sm00284b

rsc.li/soft-matter-journal

Myxococcus xanthus is a unicellular organism known for its capacity to move and communicate, giving rise to complex collective properties, structures and behaviors. These characteristics have contributed to position *M. xanthus* as a valuable model organism for exploring emergent collective phenomena at the interface of biology and physics, particularly within the growing domain of active matter research. Yet, researchers frequently encounter difficulties in establishing reproducible and reliable culturing protocols. This tutorial provides a detailed and accessible guide to the culture, growth, development, and experimental sample preparation of *M. xanthus*. In addition, it presents several exemplary experiments that can be conducted using these samples, including motility assays, fruiting body formation, predation, and elasticotaxis—phenomena of direct relevance for active matter studies.

1 Introduction

M. xanthus is a bacterium extensively used in research as a model organism. In nature, it is found in soils, close to decaying organic matter where it feeds on other microorganisms[1,2] through the production of substances that kill and lyse them externally. Some of these secreted compounds are antibiotics[3] that allow *M. xanthus* to compete with and eradicate other soil bacterial colonies[4] – a feature of particular significance in the context of the current antibiotic resistance crisis.[5] Furthermore, *M. xanthus* forms myxospores—dormant, highly resistant cells capable of surviving desiccation, starvation, heat, or chemical exposure.[6,7] Sporulation is most effective within dense groups aggregated into fruiting bodies,[8] ensuring colony survival and successful repopulation once conditions improve. These behaviors further enhance adaptability, allowing coordinated reactions and increased colony persistence compared to solitary cells.

Interestingly, both these phenomena are closely related to collective behaviors, where *M. xanthus* features a fascinating transition between unicellular and multicellular organization.[9–13]

There are biological, chemical and physical mechanisms behind its organization,[13–17] which features a complex array of strategies that allow it to adapt and thrive in different environmental conditions, as schematically shown in Fig. 1. These strategies are similar to those active matter systems feature in complex and crowded environments.[18] In nature, active matter systems can be found at all scales, from traffic jams to human crowds, schools of fishes, flocks of birds, swarms of insects, plankton communities, and motor proteins in the cytosol. There are also artificial examples of active matter like robots, Janus particles, and micromotors. Bacterial communities, such as those formed by *M. xanthus*, provide a versatile model system for studying active matter, and despite their apparent simplicity, they exhibit complex collective behaviors. Some (but not many) strains can be cultured and observed in controlled environments.[19,20]

Bacterial collective behaviors arise from at least two independent processes. First, most bacteria are able to extract energy from their environment and use it to displace themselves. This type of motility, for example, allows them to escape hostile or unfavorable conditions, greatly contributing to their survival chances. Different mechanisms exist for bacterial movement—and bacterial species can usually employ more than one, depending on environmental conditions.[21,22] Many of these motility strategies involve collective motion, which is

[a] *Department of Physics, University of Gothenburg, SE-41296 Gothenburg, Sweden. E-mail: jesus.manuel.antunez.dominguez@physics.gu.se, giovanni.volpe@physics.gu.se*
[b] *Facultad de Ciencias, Universidad Nacional Autónoma de México, Av. Universidad 3000, Circuito Exterior S/N Delegación Coyoacán, C.P. 04510 Ciudad Universitaria, D.F., Mexico*
[c] *University of Vienna, Faculty of Physics, Boltzmanngasse 5, 1090 Vienna, Austria*
[d] *Vienna Doctoral School in Physics (VDSP), University of Vienna, Austria*
[e] *Instituto de Física, Universidad Nacional Autónoma de México, C.P. 04510 Ciudad de México, Mexico*
[f] *Laboratorio Nacional de Ciencias de la Sostenibilidad (LANCIS), Instituto de Ecología, Universidad Nacional Autónoma de México, C.P. 04510 Ciudad de México, Mexico*
[g] *Science for Life Laboratory, Physics Department, University of Gothenburg, SE-41296 Gothenburg, Sweden*

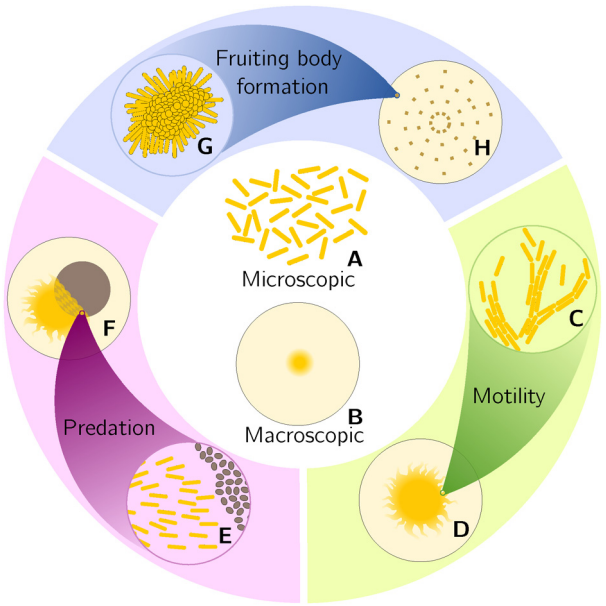

Fig. 1 *M. xanthus* colonies develop different strategies to adapt to their environment, leading to the formation of macroscopic patterns from microscopic entities. (A) Single *M. xanthus* bacteria (represented by dark yellow rods) spread randomly and moving independently from each other. (B) A freshly inoculated agar plate (light yellow circle) shows no macroscopic pattern because the bacteria are not organized. (C) Over time, the bacteria join together into swarms to more effectively explore their environment. (D) In the agar plate, the colony develops flares at the edges as a consequence of the swarming. (E) When another colony of microorganisms (brown circles) is found, *M. xanthus* organizes itself into ripples to feed on them. (F) Rippling can be seen as macroscopic waves of bacteria in the agar plate. (G) If starved, *M. xanthus* forms mound-shaped fruiting bodies to produce myxospores capable of surviving for long times in very harsh environments. (H) The fruiting bodies appear over the agar plate in regular (typically, circular) patterns.

often associated with an increased survival probability of at least one individual in the group. Second, bacteria can communicate through the secretion and detection of chemical substances, a phenomenon known as quorum sensing.[23,24] Although it occurs primarily among cells of the same species, communication between different species is also widespread. What is more, bacteria are known to communicate with other complex living beings, such as plants,[25] fungi,[26] and animals.[27,28]

By combining their activity and communication, bacteria develop emergent collective properties. Some examples are found in the coordinated movement of swarms and other cellular structures[29] for effective environmental exploration,[30,31] the realization of tasks that benefit the community rather than the individual,[32,33] and the aggregation into colonies for protection.[34]

In laboratory settings, the study of bacterial collective behavior often involves the use of fast-growing strains capable of swarming. Bacterial swarmers can be categorized into robust swarmers (*e.g.*, *Proteus mirabilis*, *Serratia marcescens*, *Bacillus subtilis*), which retain swarming behavior on rigid agar ($\geq$1.5% agar concentration), and temperate swarmers (*e.g.*, *Escherichia coli*, *Salmonella enterica*, *Pseudomonas aeruginosa*), which lose the ability to swarm at higher agar concentrations.[35] A key example is *Escherichia coli*,[36] which exhibits two primary motility mechanisms: swimming and swarming,[37] both driven by flagellar rotation. Swimming occurs in liquid media and, when performed by large groups of bacteria, can strongly affect the hydrodynamic properties of the fluid. These hydrodynamic effects of collective swimming have been extensively studied.[38–43] Moreover, depending on the timescale, bacterial movement can influence local fluid properties in submerged environments coupling motility with rheological responses.[44] In this context, the term "collective" refers to emergent patterns arising from the simultaneous activity of many cells in an active suspension, rather than to synchronization or direct communication between individuals. By contrast, synchronized swimming behaviors such as flocking[41,45,46] are comparatively rare. Swarming, on the other hand, takes place on solid surfaces.[47] *E. coli* is a temperate swarmer, restricted only on soft to semi-solid surfaces.

Another widely studied bacterium for collective behavior research is *Bacillus subtilis*,[36] a model organism for biofilm formation, which is an adaptive mechanism relying on bacterial aggregation to survive adverse conditions.[48] *B. subtilis* can form biofilms on both solid and liquid surfaces,[49] using swimming and swarming motility *via* flagella to access these environments. Similarly, *Pseudomonas aeruginosa* is a motile bacterium[50] characterized by swimming, swarming, and twitching motility, as well as biofilm formation.[51] *P. aeruginosa* is primarily studied for its role in colonizing both biotic and abiotic surfaces,[52,53] leading to infections such as cystic fibrosis and contamination of medical devices.[54] Its ability to form biofilms and its diverse motility patterns have also contributed significantly to its development of antibiotic resistance. *Vibrio cholerae* can also swarm,[55] in addition to forming biofilms[56] and swimming. Research on *V. cholerae* focuses on its role as a pathogenic colonizer in diverse environments and the spatial patterning of its colonies.[57] *Serratia marcescens* shares similar motility capabilities, with the added benefit of being a robust swarmer that forms distinctive macroscopic patterns.[58,59] However, like *P. aeruginosa*, it is a human pathogen with a high potential for developing antibiotic resistance.[60] The main advantage of these strains lies in their ease of culture. *E. coli*, *B. subtilis*, *P. aeruginosa*, and, to a lesser extent, *V. cholerae*, are well-established laboratory strains with accessible protocols that require minimal equipment and only basic microbiology knowledge. While *B. subtilis* and most *E. coli* laboratory strains are relatively safe, *P. aeruginosa*, *S. marcescens*, and *V. cholerae* pose significant infection risks, limiting their use by researchers without microbiology expertise. Additionally, these strains contribute to the growing threat of antibiotic resistance, with all of them classified by the World Health Organization as species in urgent need of new antibiotics.[61] Furthermore, most of these bacteria are temperate swarmers, displaying swarming behavior only under specific conditions. These bacteria often swim independently or join biofilms as sessile cells, limiting the observation window for coordinated motility.[62]

In contrast, *M. xanthus* is a robust swarmer capable of moving efficiently across solid surfaces. It is harmless to humans, and its antibiotic-producing properties could aid in combating antibiotic resistance rather than exacerbating it,

making it a versatile and valuable model for research of increasing interest.[2,63]

The cells are elongated and flexible (illustrated by the dark yellow rods in Fig. 1A) and motile only when on a solid surface such as on an agar plate (light yellow circle in Fig. 1B). Depending partly on the density of the population, motility can be independent, called adventurous (Fig. 1A), or inside a swarm, known as social (Fig. 1C). Swarming behavior can be recognized in the colony as branching structures of cells flowing in the same direction (such as the flares in Fig. 1D). These processes rely on different cellular mechanisms.[64] In many flagellated bacteria, swarming is coupled to the chemotaxis system,[65] which reprograms motor bias and induces hyperflagellation[66] to optimize collective expansion.[36,67,68] For instance, *E. coli* swarmers reduce tumble bias and increase speed, while in *B. subtilis* swarming depends on surfactant production and specialized tip populations.[69] By contrast, *M. xanthus* swarms *via* type IV pili–driven gliding and slime secretion, independent chemotaxis regulation. Swarming dynamics are strongly substrate-dependent: flagellated swarmers reach >40 μm s^{-1} on soft agar but slow down to 2–10 μm s^{-1} on rigid agar,[70] whereas *M. xanthus* achieves 20 μm min^{-1} on 0.3% agar and 6 μm min^{-1} on firmer agar.[71] Notably, *M. xanthus* motility systems adapt differentially to surface stiffness, with higher agar concentrations favoring adventurous motility and lower concentrations promoting social motility.[72]

During extended growth (up to 48 hours), *M. xanthus* forms biofilms supported by an extracellular matrix (ECM) of polysaccharides, proteins, fibrils, and extracellular DNA. The ECM provide cell–cell cohesion,[73,74] while DNA–exopolysaccharide conjugates stabilize the biofilm and enhance stress resistance.[75] Proteomic studies show enrichment of secreted proteins linked to aggregation and fruiting body development.[76,77] ECM production is also coupled to motility *via* type IV pili.[78] The ECM benefits *M. xanthus* by protecting cells, enabling coordinated multicellular behaviors, and supporting fruiting body formation. Beyond ECM, the species gains ecological advantages from its predatory lifestyle: it disrupts pathogenic bacterial biofilms[79] and efficiently hunts prey across varied ecological conditions, with prey type, density, and surface properties strongly influencing predation efficiency.[80,81]

Another example of collective behavior can be found in its predatory strategies. *M. xanthus* is an epibiotic predatory bacterium:[82] when exposed to colonies of other microorganisms, it approaches them and secretes antibiotics and enzymes to feed on them (Fig. 1E). The whole population associates and organizes in ripples to enhance its efficiency (Fig. 1F). When the conditions are no longer favorable for exploration or predation, the community undergoes a change. Some of the cells turn into myxospores inside protective structures known as fruiting bodies (Fig. 1G) that distribute throughout the agar surface (Fig. 1H). The formation of myxospores and fruiting bodies may not beneficial for single cells but to the full community.[83,84] This has been proposed as an example of cooperative behavior, where the focus of preservation shifts from the individual to the community[85] as well as an example of a transition from unicellular to multicellular life.[13] The myxospores in a fruiting body will germinate into a swarm if the conditions become favorable again, restarting the life cycle.

The variety of collective behaviors along its life cycle has spurred the interest in *M. xanthus*. Nonetheless, laboratory culture of this species requires several steps, including solid cultures in agar plates and liquid cultures in a nutritious medium. Additionally, their survival and development demand specific conditions of sterility, humidity, temperature,[14] and light.[86,87] Successfully preparing and properly handling bacterial samples require training that might be missing in an interdisciplinary laboratory with a focus towards chemistry or physics, which constitutes a potential barrier to the study of these systems by researchers without a strong bacterial biology background. However, the primary challenge with using *M. xanthus* as an experimental subject is its slower growth rate. Techniques effective for other bacterial strains often do not yield consistent results with *M. xanthus*. Specific methods are needed to ensure reliable experimental samples, but such information is not widely available, especially for researchers without a specialized microbiology background.

The value of *M. xanthus* extends beyond active matter into quantitative biology, an interdisciplinary field that combines biology, physics, mathematics, and computer science to analyse complex systems. Owing to its social behaviors and developmental programs, *M. xanthus* is a tractable model for connecting experiment and theory. Quantitative approaches have shown, for example, that cell-tracking combined with simulations can capture collective motion without detailed molecular knowledge, revealing mechanisms such as reduced motility within clusters, directed motion toward aggregate centers, and alignment with neighbors.[88] Similarly, fruiting body formation has been described as a phase-separation process, with cells tuning their motility over time.[89] Additional studies have examined signaling networks and developmental dynamics underlying cooperation and pattern formation.[90,91] A clear, standardized tutorial on culturing *M. xanthus*, which is not currently available, would support researchers in conducting rigorous studies, bridging the gap between microbiology and quantitative biology. In this tutorial, we offer a straightforward, step-by-step guide for the culture and growth of *M. xanthus*, tailored for interdisciplinary researchers without a strong background in bacterial biology. Additionally, we provide examples of possible experiments to be performed with *M. xanthus*. Beyond covering the basics, we also provide tips and tricks that often do not find place in published articles, maximizing reproducibility.

2 Culture procedure

In this tutorial, we present standard protocols relevant to general microbiology in the SI—namely, SI: 2.2 Autoclaving, SI: 2.3 Preparation of Erlenmeyer flasks with liquid media, and SI: 2.4 Preparation of agar plates—while protocols specific to the culture and experimentation with *M. xanthus* are described in the subsequent sections. The complete growth process of

M. xanthus culture is portrayed in the timeline in Fig. 2. We propose the weekly schedule described in Table 1, in which a new colony from a frozen stock is revived at the end of every week to be used in experiments during the following week. Agar cultures are used at the beginning for the recovery of a viable population from the frozen stock. For experiments, liquid culture is preferred to assess population density according to OD_{600} (optical density at 600 nm illumination wavelength) measurements with reference to a blank sample of sterile growth medium. Measuring OD_{600} over time allows the generation of a bacterial growth curve,[92] typically divided into four phases: lag (adaptation to the medium), log or exponential (rapid binary division), stationary (cell division balanced by death), and death (population decline). These phases are influenced by nutrient availability and accumulation of waste products in the culture medium. Growth curves for *M. xanthus* can be found in ref. 93–96, and the relationship between OD_{600} and colony-forming units (CFU) as an estimate of cell or aggregate number is detailed in ref. 97. CFU can be determined by different means like microscopy[98] or by the spread plate method.[99]

While alternative wavelengths for measuring optical density, such as OD_{550}, are sometimes used to minimize interference from the yellow pigments produced by *M. xanthus* cultures,[13] OD_{600} remains the widely adopted standard, ensuring consistency and comparability across studies. The relation of OD to cell counts has been established in previous work.[97] Cell growth can lead to changes in cell length; however, this will not be addressed here, as most assays were performed in starvation medium where division is negligible. This factor becomes relevant under nutrient-rich conditions.

Every day, a 24-hour concentrated liquid culture is obtained and used both for experiments and as the inoculum for the following day's culture, resulting in five independent experiments per week. After five days of experiments, the culture is discarded, and a new solid culture inoculated from a frozen stock is started.

M. xanthus is a soil dwelling bacterium completely harmless to humans. *M. xanthus* can be found globally[100] and has been isolated from a wide variety of soils containing decaying organic matter,[101,102] underscoring the ecological success of its cooperative lifestyle. The widely used laboratory wild-type strain DK1622 of *M. xanthus* was specifically employed for the procedures outlined in this tutorial. This strain serves as a robust starting point that may be applicable to other strains, including those isolated from natural environments.[102] However, other strains and related species may exhibit variations in development times, temperature preferences, and growth media. The methods established here provide a framework for developing a culture pipeline specifically for *M. xanthus*. The proposed materials and equipment represent a cost-effective yet reliable starting point for initiating cultures of this bacterial strain. The required equipment is largely basic, widely available, and typically accessible in standard laboratory facilities. More advanced or specialized instrumentation may be incorporated following a favorable initial assessment and if further investment is feasible.

The wild-type strain of *M. xanthus* is non-pathogenic; therefore, the facilities required for this research must comply with biosafety level 1 (BSL-1) standards.[103] Under these conditions, safety measures are not restrictive, and work benches may be in open laboratory spaces. The primary requirements include thorough handwashing before and after handling biological material, prohibition of eating, drinking, or smoking within facilities dedicated to this research, and routine decontamination of surfaces and materials that come into contact with biological specimens. Waste should be disinfected prior to disposal, preferably by sterilization in an autoclave when the material is compatible. Afterwards, it can be safely discarded with combustible waste.

The presence of its spores can contaminate tools and surfaces. Consequently, it is critical to properly sterilize and dispose of contaminated material. The work space was wiped with ethanol at 70% concentration and kept safe from contamination during sample handling using a burner represented in Fig. 3A.

Reusable tools, glass and metallic, are dipped in ethanol and the excess is burned for two minutes in the flame. Metallic tools

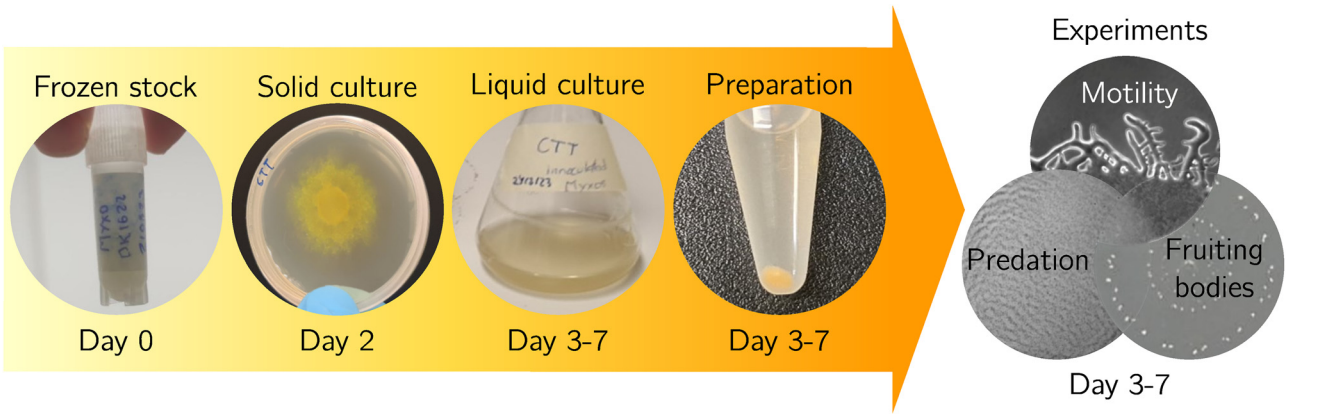

Fig. 2 Steps for the culture of *M. xanthus*. From a long term storage glycerol stock, an initial solid culture is required to develop a viable colony. This colony is then transferred to liquid medium for better assessment of cell concentration through optical density (OD_{600}) for experiment repeatability during each day of the week. After centrifuging and resuspending, cells can be used in experiments. Here, we focus on three main phenomena: motility of the community and cells, predation of other microbial colonies, and formation of fruiting bodies in adverse environmental conditions.

Table 1 Proposed schedule for *M. xanthus* culture. A new plate is inoculated on the first day to be used during five days of experiments. The "Requirements" column indicates what is needed in advance. The "Activity" column refers to the relevant sections of this tutorial. The "Results" column indicates the outcome of each activity, organized to match the requirements of the next day

Day	Requirements	Activity	Result
In advance	Material & reagents stockage	Preparation of culture media	CTT plates CTT flasks TPM plates
Day 1	CTT plate Frozen stock	From frozen stock to agar plate	Inoculated CTT plate
Day 3	Grown colony plate CTT flask	From agar plate to liquid medium	Inoculated CTT flask
Day 4	CTT flask TPM plate Overnight culture flask	Liquid culture continuation Experiments If few frozen stocks are left: liquid medium to frozen stocks	Inoculated CTT flask Experimental data Frozen stocks
Day 5	CTT flask TPM plate Overnight culture flask	Liquid culture continuation Experiments	Inoculated CTT flask Experimental data
Day 6	CTT flask TPM plate Overnight culture flask	Liquid culture continuation Experiments	Inoculated CTT flask Experimental data
Day 7	CTT flask TPM plate Overnight culture flask	Liquid culture continuation Experiments	Inoculated CTT flask Experimental data
Day 8	TPM plate Overnight culture flask CTT plate Frozen stock	Experiments From frozen stock to agar plate	Experimental data Inoculated CTT plate

should turn red hot during the process. Otherwise, tools can be disinfected by soaking them for at least 15 minutes in 70% ethanol. Alternatively, disposable tools must come in a sterile packaging and open only in a clean environment. Contamination of fast-growing species is one of the main obstacles found during culture. Other bacteria can affect the growth of *M. xanthus* by producing waste and depleting resources in both solid and liquid cultures. The *M. xanthus* culture should be handled with gloves in a clean environment to avoid contamination from spores or airborne bacterial species. A laminar flow hood or a burner are recommended to maintain a clean working area. The latter will be used in this tutorial to minimize equipment requirements. The list of all the materials needed for this tutorial can be found in the SI: 1.2 Material tables.

To ensure reproducibility, the protocol of this tutorial was also replicated in a second laboratory (the primary laboratory is at the University of Gothenburg, while the second laboratory is at the University of Vienna), where different equipment was employed (see SI: Table S1 and SI: Table S2 respectively). In particular, in this second laboratory neither a laminar flow hood nor a burner were used but a PCR UV cabinet instead.

All consumable items required are listed in SI: Table S3, while all reagents and medium recipes are in SI: Table S4 and SI: Table S5, respectively.

Throughout this tutorial, two media are used for the handling and growth of *M. xanthus*. A step-by-step guide on how to prepare them can be found in the SI: 2.1 Preparation of liquid media as well as a guide on how to sterilize them using an autoclave in the SI: 2.2 Autoclaving.

For the culture and growth of *M. xanthus*, we use CasiTone Tris (CTT) medium, which contains a buffer with added peptone casitone for nutrition. A peptone is the result of the partial breakdown of a protein into its constituent amino acid chains. In the case of casitone, the protein casein is broken down by animal pancreatic enzymes into chains of different sizes. The result is a supplement with variable composition, as opposed to a chemically defined medium, but with all the necessary components for bacterial growth. CTT is required as both liquid medium and agar plates to culture *M. xanthus*, but it can also be used in motility experiments on agar plates.

Tris phosphate magnesium (TPM) buffer is a solution that is used to keep the pH stable during bacterial development. Since it lacks any nutritional value but provides a stable environment, it is used to induce starvation conditions. TPM is used in liquid form only during sample preparation, and as agar plate during most experiments to induce starvation, encouraging motility, predation and fruiting body formation.

When properly sealed and maintained sterile, autoclaved media can be stored at room temperature, protected from direct sunlight and large temperature fluctuations. While TPM buffer can be viable and stored for more than a year, CTT medium should be used within 3 to 6 months before protein degradation. The medium should be clear yellow, hence turbidity or changes in the color of the media are signs of degradation and contamination, leading to their disposal. To use CTT medium as a liquid culture, it was prepared in Erlenmeyer's flasks secured with caps made out of cotton, gauze and tape (Fig. 3B). The cotton is enveloped by the gauze as shown in Fig. 3C and held in place by the tape (Fig. 3D). These caps provide a window for air circulation without risking contamination of the culture. The step by step guide on how to prepare the liquid culture flasks can be found in the SI: 2.3 Preparation of Erlenmeyer flasks with liquid media.

To prepare solid media, agar is added in the proportion of 1.5%, expressed as mass of solute over volume of solution, that

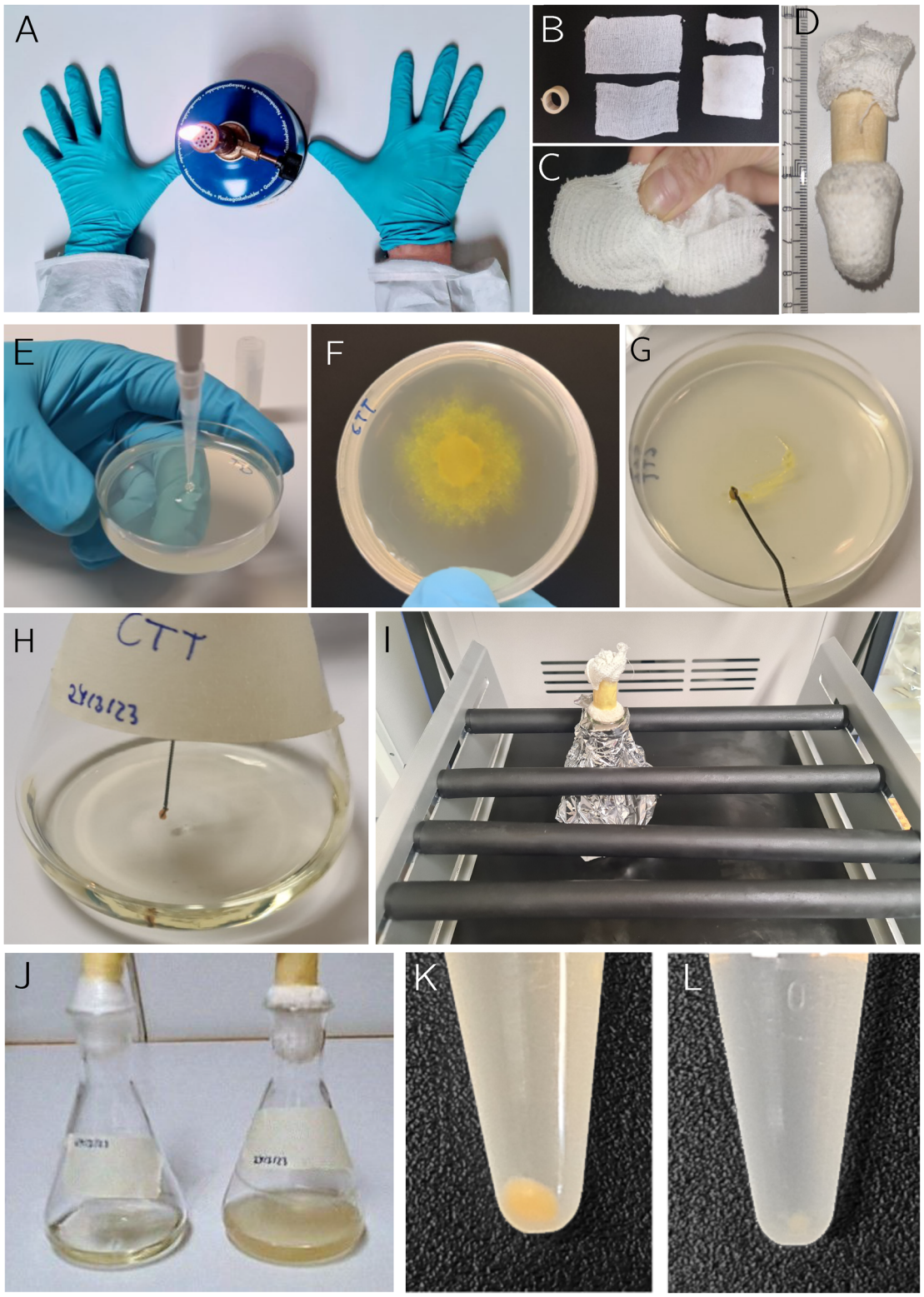

Fig. 3 Main steps for the culture of *M. xanthus*. (A) Approximation of the clean working space provided by a burner. (B) Materials used in the fabrication of cotton caps for liquid cultures, including gauze, cotton and tape. (C) Assembly of the materials of the cotton cap. The cotton is shaped into a ball, placed in the middle of two superposed squares of gauze and wrapped tightly by joining all the edges and corners of the gauze. (D) Finished cotton cap after securing with tape. (E) Inoculation of a CTT agar plate with *M. xanthus* from a frozen stock. (F) CTT agar plate with a colony grown for 48 hours. (G) Scrapping the full colony using an inoculation loop. (H) Inoculation of liquid medium with a colony from a CTT plate. (I) Placement of the liquid culture flask in the shaker incubator, covered with aluminium foil. (J) Comparison of turbidity of an sterile CTT medium flask *versus* a proliferated CTT flask ready to use in experiments. (K) Pellet of a centrifuged sample of *M. xanthus* for dense population experiments (OD_{600} = 0.5). (L) Pellet of a centrifuged sample of *M. xanthus* for sparse population experiments (OD_{600} = 0.05). Illustrated here are the basic methods described in the tutorial, as an initial step for introduction to the culture of *M. xanthus* with minimal investment in new resources and capitalizing on materials readily available in most laboratories.

is, 15 g of agar powder for 1 L of liquid medium. A guide describing in detail the process to produce agar plate of the desired medium can be found in the SI: 2.4 Preparation of the agar plates. When properly sealed, sterile agar plates, can be stored in the same conditions as the liquid media for up to 3 months for culture continuation. However, for experiments, fresh agar plates are advised to ensure an accurate water content. A decrease in the level of the agar and the appearance of unknown colonies indicate inefficient sealing of the plates, rendering them inadequate for use.

Frozen stocks are used for long term storage of bacterial strains, lasting for more than a year while kept at −80 °C. To recover a healthy viable colony of *M. xanthus*, they are first inoculated in an CTT agar plate at optimal conditions, considering temperature and no light exposure, as seen in Fig. 3E and detailed in in the SI: 2.5 From frozen stock to agar plate. "*M. xanthus* optimal growth occurs at approximately 32 °C.[14] Although capable of proliferating at lower temperatures, colony growth—but not cell morphology or collective behavior—will be severely affected. In contrast, temperatures above 36 °C impose stress, resulting in aberrant morphology.[104] Thus, culturing at 32 °C ensures maximal growth and normal cellular physiology while minimizing stress-related artifacts in experimental studies.

In the agar plate, the bacteria will grow and spread unevenly over the surface as shown in Fig. 3F. Solid cultures allow for easy detection of the characteristic features of an *M. xanthus* colony, such as color, shape, and texture. The solid culture therefore serves as an initial visual check for contamination or significant random mutations in the population. Additionally, frozen cells from glycerol stocks need to stabilize and increase in density before they are ready for growth in liquid medium. Since *M. xanthus* is a gliding bacterium, the physicochemical properties of agar substrates more closely resemble those of its natural niche than the liquid environment. Nevertheless, solid support is inconvenient for extraction and quantification of cells. Therefore, the colony is scraped as shown in Fig. 3G and transferred in liquid culture (Fig. 3H), which allows monitoring cell concentration *via* optical density measurements. However, since *M. xanthus* is unable to swim, the culture must be shaken to maintain the bacteria in suspension. This whole process is explained in more detail in the SI: 2.6 From agar plate to liquid medium.

M. xanthus will actively grow in liquid culture if protected from light and at 32 °C, as seen in Fig. 3I. Over time, the community will stagnate due to nutrient depletion while accumulating a significant amount of dead cells and waste material. This will affect the viability of the samples and reliability of concentration measurements. To ensure the repeatability of experiments, a new liquid culture is started every day to be used on experiments the next as shown in Fig. 3J and explained in the SI: 2.7 Liquid culture continuation.

After obtaining successful growth of any strain of bacteria, it is convenient to secure a viable population for future experiments. Here, we include instructions for long term storage by making glycerol stocks in the SI: 2.8 Liquid media to frozen glycerol stocks that must be kept at −80 °C. The resulting glycerol stocks are ready to use and can last for years.[105] Each one can be used multiple times; nevertheless, each thaw-freeze cycle will decrease the viability of the extracted inoculate. Glycerol stocks of the same batch come from a homogeneous population and are less susceptible to variations. Therefore, it is recommended to produce many glycerol stocks of the same culture to be stored and used over long periods of time rather than frequent production of stocks that might accumulate variations over time. Glycerol stocks are also the preferred means of shipping if kept at −80 °C. Otherwise, it is preferable to send recently inoculated agar plates that must be transferred to liquid medium on the day of arrival.

Having obtained grown liquid cultures of *M. xanthus* in CTT, samples must be prepared to be used. The CTT medium leftovers must be washed to not interfere with the starvation conditions of most experiments. Additionally, the population density was assessed through the OD_{600} for repeatability as detailed in the SI: 2.2 Washing samples for experiments. Population density is adjusted by extracting bacterial suspension and diluting with clean CTT until the desired concentration is reached. Here, two population densities are considered: dense population samples have an OD_{600} of 0.5, while the sparse population samples have an OD_{600} of 0.05. However, this parameter can be adapted and tuned according to the need of each experiment. In Fig. 3K and L, see the contrast between the resulting pellets of a concentrated and diluted sample, respectively. In the latter, the pellet might not be visible by naked eye.

3 Experiments

This section showcases some experiments that can be performed with *M. xanthus* to give an overview of the potential research topics that can be studied with this model organism. Each of the experiments described below is independent and primarily serves as a demonstration to illustrate the potential of *M. xanthus* for active matter studies, rather than as a comprehensive investigation aimed at generating novel biological findings.

Detailed specifications for experiment design are beyond the scope of this paper. In particular, the image acquisition procedures will depend on the specifics of each optical setup (for example, the use of an inverted or non-inverted microscope, or the access to temperature and humidity control with a stage incubator). The main challenges to overcome are condensation in the optical window, agar water loss over time, and agar evenness. Microscopic observation was performed using confined agar systems in which cells were kept between two glass coverslips separated by a plastic gasket, following the protocols in the literature.[106,107] This configuration preserves the standard cover-slip thickness and is compatible with high-magnification objectives, including immersion lenses. To prevent evaporation and maintain agar consistency over long-term recordings (up to 96 hours), the chambers were sealed with vacuum grease, ensuring a constant vapor pressure within the sample environment. Reliable long-term monitoring of cell

dynamics required continuous focus correction or autofocus to compensate for drift in both Petri dish and *in situ* chamber setups. All experiments were conducted in microscope incubators that controlled temperature and humidity, thereby ensuring reproducible growth conditions and stable imaging over several days. For short-term, community-scale colony observations, Petri dishes were used (SI: 3 Petri dish adaptation for observation), whereas long-term, high-magnification imaging was always performed in sealed chambers.

To broaden the spectrum of motility studies, fluorescent labeling of bacteria can be employed. Although not implemented in the present tutorial nor required for the described analyses, we note these approaches here for completeness. Protocols using dyes to stain the extracellular matrix[108,109] or live/dead staining[110] to study predation interactions have been established to characterize *M. xanthus* behavior, facilitating detailed observation of motility patterns and interactions in real time. More advanced approaches involve tagging with fluorescent proteins,[111–114] enabling tracking of single cells within the community.[115]

3.1 Motility

One of the primary applications of bacterial motility in active matter research is targeted delivery. By modifying environmental conditions, exploiting intrinsic motility mechanisms, and applying genetic modifications, microbes can be directed toward specific targets.[116] Additional *M. xanthus* capabilities, such as cargo encapsulation[117] and colony detection,[118] further enhance their potential for targeted delivery. Bacterial colonies also serve as natural examples of active nematics,[19] *i.e.*, systems composed of rod-like active matter.[119,120] Collective behaviors such as biofilm formation,[121] colony expansion,[122,123] and swarming have been interpreted within the framework of active nematics. In *M. xanthus*, dense colonies remain largely planar, providing a natural instance of a two-dimensional active nematic system,[124] with additional features such as alternating motility systems and crystal-like arrangements. These emergent patterns of collective behavior not only inform fundamental studies of active matter but also underpin practical applications in which coordinated bacterial movement is essential.

The investigation of the motility of *M. xanthus* also opens significant opportunities for environmental remediation and biotechnological innovation.[125] Ecological applications of *M. xanthus* include its potential use as a biocontrol agent,[126] its ability to partially degrade organic matter through enzymatic activity, and its role in the biomineralization of metals and pollutants. However, unlike bacteria such as *Rhizobium*,[127] which are used as biofertilizers due to their ability to fix nitrogen,[128] *M. xanthus* does not perform such specialized functions.[129] The identification of a novel biosurfactant polysaccharide (BPS)[130] in *M. xanthus* highlights its role in swarm migration, biofilm formation, and fruiting body development, suggesting potential for bioremediation akin to *Acinetobacter* sp. RAG-1, which produces an emulsifying compound effective in oil and heavy metal remediation.[131] Furthermore, *M. xanthus* can neutralize artificially acidified soil through its metabolism, generating ammonium ions and hydroxide.[132] The bacterium has also been found to interact with metals such as copper[133] and silver,[134] illustrating its potential for recycling valuable metals from low-concentration solutions and emphasizing its adaptability to varying environmental conditions. *M. xanthus* is known for its ability to biomineralize and precipitate different minerals depending on the medium composition.[135,136] This phenomenon has been utilized in practical applications such as bioremediation of nuclear elements like uranium and the protection of carbonate stone structures.[137,138] Overall, the unique biomineralization capabilities of *M. xanthus* not only play a crucial role in biogeochemical cycles but also pave the way for innovative applications in sustainable technologies such as producing the scaffold to support complex bacterial communities.[136] The study from the perspective of active matter is essential for optimizing the development of these applications, as it addresses key aspects such as population spread and their impact on reaction efficiency and crystal size.

Beyond characterizing solitary and collective gliding, such models can inform broader aspects of bacterial–environment interactions. Recent work has shown that gliding systems may shed light on flow interactions,[139] the ability of microorganisms to sense and respond to chemical gradients,[140] and the relevance of soil-mimicking environments (soil-on-chip[141,142]) for understanding motility in natural habitats.[143] Such systems are particularly useful for studying microbial communities and their interdependence, providing insights into the so-called microbial dark matter.[144,145]

M. xanthus requires a solid surface for displacement. On hard agar (1.5%), bacterial gliding does not involve propulsion through a bulk viscous fluid. Nevertheless, based on cell size and velocity, the motion is characterized by a low Reynolds number, where dissipative forces dominate over inertia. An estimate for the case of *M. xanthus* can be found in SI: 4 Reynolds number approximation. Similar low-Re gliding has been reported for bacteria moving through slime.[146–148]

Looking at the full colony development on CTT agar plates over the course of days, one can observe pigment production (DKxanthene[149,150]) as well as displacement of swarms from the original inoculation site, as shown in Fig. 4A. In the presence of light, different pigments will be produced and *M. xanthus* growth will be affected.[86] In contrast, in TPM agar plates, no pigment is produced and the colony remains almost invisible to the naked eye. Depending on the spatial scale of observation, different time scale should also be considered.

The collective behavior of a section of the bacterial colony can be monitored for hours to analyze the displacement of swarms, as shown in Fig. 4B. After 48 hours of incubation on CTT plates, regions of pigment accumulation and crystal formation become visible (see Video S1). These crystals are struvite, formed due to the precipitation of the ammonia waste produced by *M. xanthus* with the magnesium ions and phosphate in CTT.

At the microscopic scale, the organization and orientation of each cell can be observed over minutes. Two kinds of motility come into focus. When isolated, cells move according to

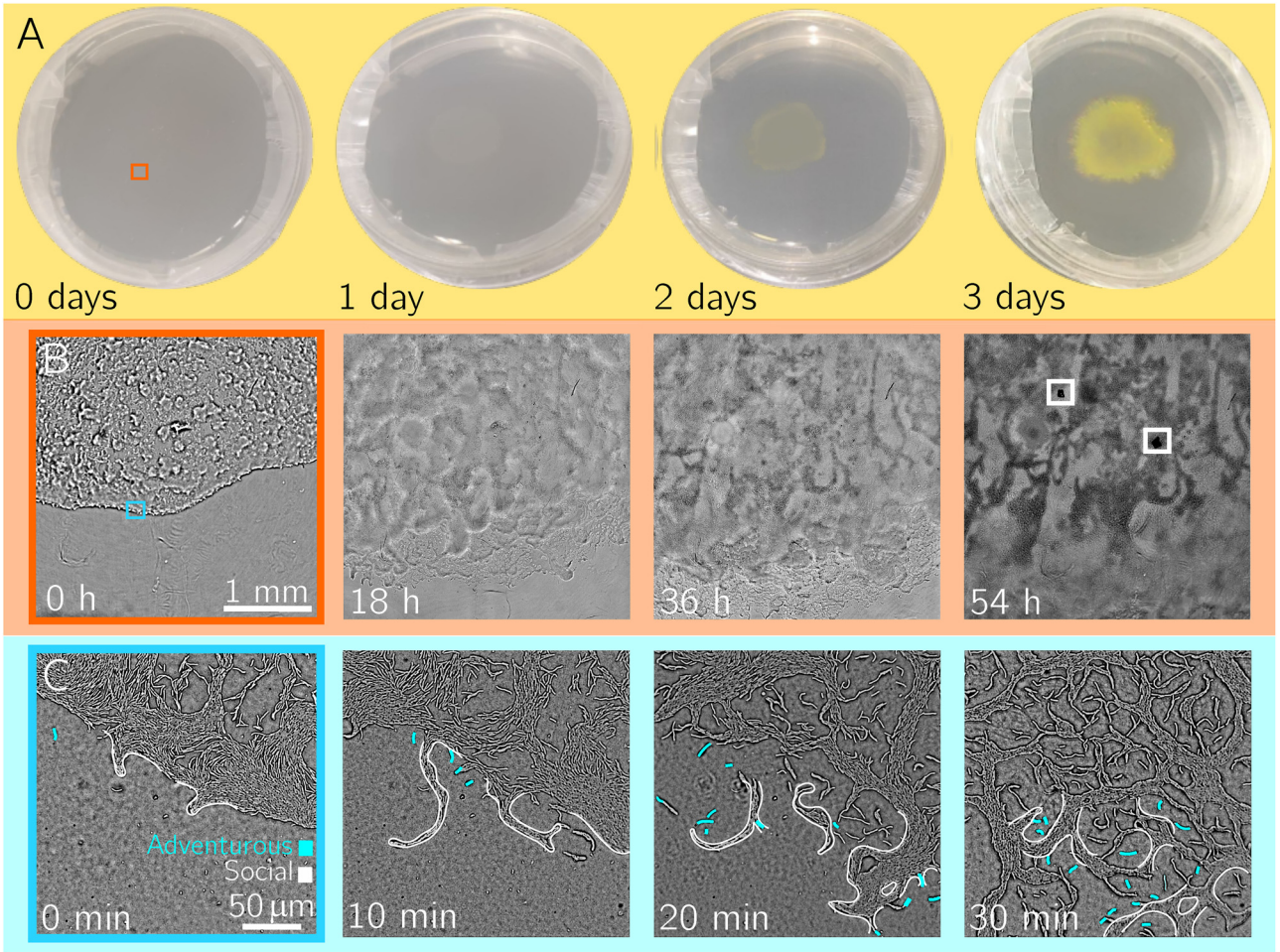

Fig. 4 *M. xanthus* motility at different spatial and temporal scales. (A) Full colony behavior on a CTT agar plate followed over the course of 3 days at 32 °C, where the production of pigment intensifies and the swarm spreads through the plate. The full Petri dish (55 mm diameter) is shown over a black background to highlight the colonies. (B) Section of the community followed for 54 hours to detect the displacement of swarms. Darker zones are due to pigment accumulation and struvite crystals are highlighted at 54 hours. Images at 4× objective magnification. (C) Microscopic view of a monolayer of cells moving forward in the course of 30 minutes. The two types of motility as highlighted at the edge of the colony. Social motility leads to the formation of flares, while events of adventurous motility can be identified in single scout cells. The images were taken at 63× objective magnification.

adventurous motility, while in high concentration, social motility will be predominant leading to the formation of swarms[151] (see Videos S2 and S3, respectively). In the latter case, cells will form swarms leading to expanding fronts in the colony known as flares[15,152,153] seen in Fig. 4C (and Videos S4 and S5). Still, some individual cells might sometimes leave the swarm to explore the environment through adventurous motility. The rigidity of the medium affects both motility mechanisms and so, different concentrations of agar will yield different results.[17,154,155]

To perform these experiments, a droplet of 13 μL of *M. xanthus* at the desired concentration should be placed on the surface of a TPM or CTT agar plate and allowed to dry. For macroscopic observations, images should be taken every hour over a total duration of 48 hours. For microscopic observations, images should be captured every 2 to 10 minutes over a total duration of 24 hours.The suggested times are only an orientation and development might still vary from one experiment to another.

In SI: 5 Bacterial tracking, we provide the manually tracked trajectories of 10 bacteria exhibiting adventurous motility. The duration, displacement and speed are analyzed through manual tracking over the timelapses of Video S4, including all observed instances of cell reversals before joining back into a swarm. These results are consistent with literature values for a mean speed of 2 μm min^{-1}.[71] In TPM (starvation medium), cell division is negligible and can be disregarded in motility experiments. However, a generation time of ≈4 h should be considered if experiments are performed in CTT.[113] We also observe back-and-forth reversals during solitary gliding, while collective motion exhibits alignment, streaming and merging into swarms, consistent with prior descriptions of coordinated gliding.

3.2 Fruiting bodies

The development of specialized latent cells for survival under harsh conditions is common among bacteria, such as endospores in Firmicutes and myxospores in *Myxococcales*. Despite their shared low metabolic activity and stress resistance, these resting cells exhibit unique morphological and chemical

signatures that must be studied to understand their functions.[156] Fruiting bodies are the defensive structures where the cells of *M. xanthus* congregate and some of them differentiate into myxospores in a phenomenon known as sporulation.[149,157,158] Spores are impervious to extreme conditions and ensure community survival if the environment turns hostile. In *M. xanthus*, fruiting body formation is highly dependent on environmental conditions and collective behavior. Fruiting body formation occurs during the natural development of *M. xanthus* but their formation can also be triggered by different means:[159–161] a decrease in humidity, an increase of certain chemical species, such as glycerol, or as in the example of this tutorial, starvation. Once these structures are formed, compounds like polyphosphates help manage energy during nutrient depletion, and their absence negatively impacts spore germination and viability.[162,163] Additionally, environmental conditions influence the production of exopolysaccharides, which play a crucial role in fruiting body formation.[5] The transition from swarming to fruiting body formation, regulated by

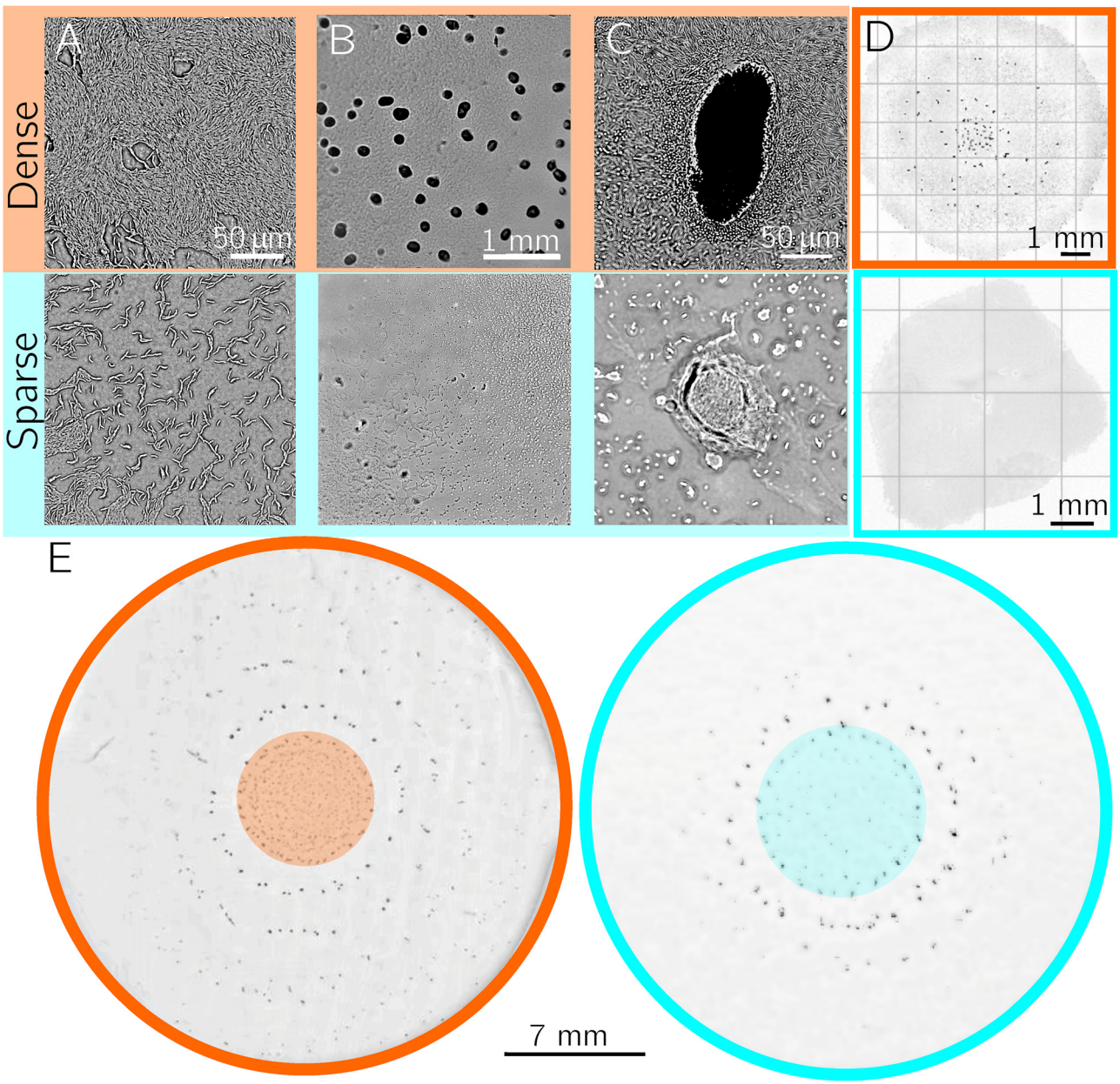

Fig. 5 Fruiting body formation (A) dense and sparse populations on TPM agar plates at the initial time point observed at 63× objective magnification. (B) Fruiting body formation at 4× objective magnification after 90 hours. (C) Close-up of a fruiting body at 63× objective magnification. (D) Comparison of the colony spread and fruiting body formation at 90 hours depending on the initial population density. The images result from the merging of adjacent pictures at 4× objective magnification. (E) Concentric pattern of fruiting bodies after one weeks incubation. The fruiting bodies of dense and sparse populations are highlighted in black. The initial inoculation site of each population is at the center of the first ring, highlighted in color. The fruiting bodies are shown against a light background.

environmental cues and quorum sensing, has itself been compared to phase transition phenomena.[89] Similar comparisons have also been made for other collective behaviors, such as biofilm formation.[34,164–166] The role of physical mechanisms, including the shift from planar to three-dimensional structures,[167,168] remains an open question in active matter studies.[89] The morphology of these fruiting bodies is theorized to affect spore resistance, offering varying degrees of protection against environmental stressors like UV radiation and desiccation.[169] A key aspect of *M. xanthus* response to harsh conditions is cellular differentiation, leading to the formation of distinct cell types within the fruiting body, vital for survival.[170] The spore germination process is also social, influenced by molecules such as glycine betaine, which facilitate cooperation among strains and allow for potential "cheating".[171] These behaviors are essential in sociomicrobiology, a field that examines population dynamics and interactions.[32,172,173] Given the context of the antibiotic resistance crisis, where collaboration promotes horizontal gene transfer and the survival of resistant colonies, understanding these dynamics could inform the development of dispersal mechanisms[174] that enhance sterilization techniques. Such advancements could mitigate the development and spread of antibiotic resistance.

In this tutorial, we will show that population density has a significant impact on the formation of fruiting bodies as demonstrated in previous works in the literature.[89,175] We compare two different population densities, designated as "dense" and "sparse", with an OD_{600} of 0.5 and 0.05 respectively, shown in Fig. 5A. In the dense population, cells are evenly distributed in layers[124] (see Video S6) with few empty spaces, while in the sparse case, most cells are isolated with most of the agar remaining empty.

After 90 hours, fruiting bodies are considerably more abundant and developed in the dense population (see Videos S7 and S8) as opposed to the sparse one (see Video S9), as shown in Fig. 5B. Comparing both videos, it can be observed that fruiting body formation strongly depends on population concentration and time. Dense populations initiate fruiting body formation around the 48-hour mark, whereas sparse populations do not form any fully-grown fruiting body within the full duration of the video. Fruiting body formation is therefore delayed at lower concentrations and may require up to a week to develop fully at the inoculation site. A microscopic look on individual fruiting bodies allows to identify myxospores, recognized by their round shape (see Video S10). They can be found mainly in the center of the fruiting body stacked on each other, even though there are also myxospores scattered around the nearby area. Vegetative cells, in the shape of elongated rods, are distributed mostly in a layer and around the fruiting body, forming a structure called haystack.[158,176,177] Not all cells will undergo differentiation in the fruiting body, as some remain to prey on possible targets or even sacrifice to sustain the sporulation process.[83,178] The fruiting bodies in a sparse population lag in growth and development when compared to those in a dense population, as shown in Fig. 5C.

In the sparse colony, adventurous motility will predominate at the beginning, leading to a slower spread of the colony in hard agar (1.5% w/v), like in Fig. 5D (while the opposite will be true for soft agar[154]). If incubated for a couple of weeks, *M. xanthus* fruiting bodies will appear at the edge of the inoculation site[9,17] and periodically in concentric lines around the original culture as shown in the plates in Fig. 5E. This ring-like organization has not been previously reported for *M. xanthus*, but has been observed in the related species *M. macrosporus*, where it is more pronounced.[179] Such pattern is not present in the inoculation site, that is, the confines of the original inoculated droplet (where the fruiting bodies positions are random), but instead outside, due to the population propagation.

To perform these experiments, a droplet of *M. xanthus* should be placed on the surface of a TPM agar plate and allowed to dry. For macroscopic observations, images should be taken every hour for a total duration of 96 hours, comparing results across different concentrations (OD) of *M. xanthus*. For microscopic observations, images should be taken every 2 to 20 minutes over the same 96-hour period. Keep in mind that times are orientative and fruiting body formation can take up to 48 hours to begin after inoculation.

The resulting colony will grow significantly, making it challenging to image the entire area or predict where fruiting bodies will form. It is recommended to capture several frames around the perimeter of the original droplet, where cell accumulation is visible, as well as a frame in the center of the inoculation droplet. These areas are where fruiting bodies are most likely to develop.

As an example of the significance of fruiting body patterning, a comparison was made between the concentric pattern formation of fruiting bodies in dense and sparse populations after two weeks of development on TPM agar. The data and procedure can be found in SI: 6 Fruiting body analysis. Fig. 6A displays the resulting patterns of a dense bacterial colony (top row) *versus* a sparse colony (bottom row). The fruiting bodies in the dense colony were more distinct and easily identifiable, with several concentric rings visible to the naked eye.

To quantify this pattern, fruiting bodies were segmented and measured using a threshold-based approach. Fig. 6B presents the distribution of fruiting body area as a function of distance from the inoculation center, illustrating their arrangement in rings. While fruiting bodies were distributed throughout the colony, gaps were present, and larger fruiting bodies tended to cluster at similar distances, reinforcing the ring-like structure. In contrast, smaller fruiting bodies were more randomly positioned and did not align as clearly with the concentric rings.

To determine the periodicity of the rings, the weighted mean position of fruiting bodies within visually identified intervals was used to estimate ring radii. In the dense population, the rings were evenly spaced at approximately 2 mm for dense populations, suggesting a consistent pattern. However, in the sparse population, spacing was much less prevalent, though it could still appear sporadically across replicates.

To assess potential commonalities among fruiting bodies, a statistical analysis of those within each ring was performed, as shown in Fig. 6C. At the colony center, fruiting body formation differed between dense and sparse populations: dense populations

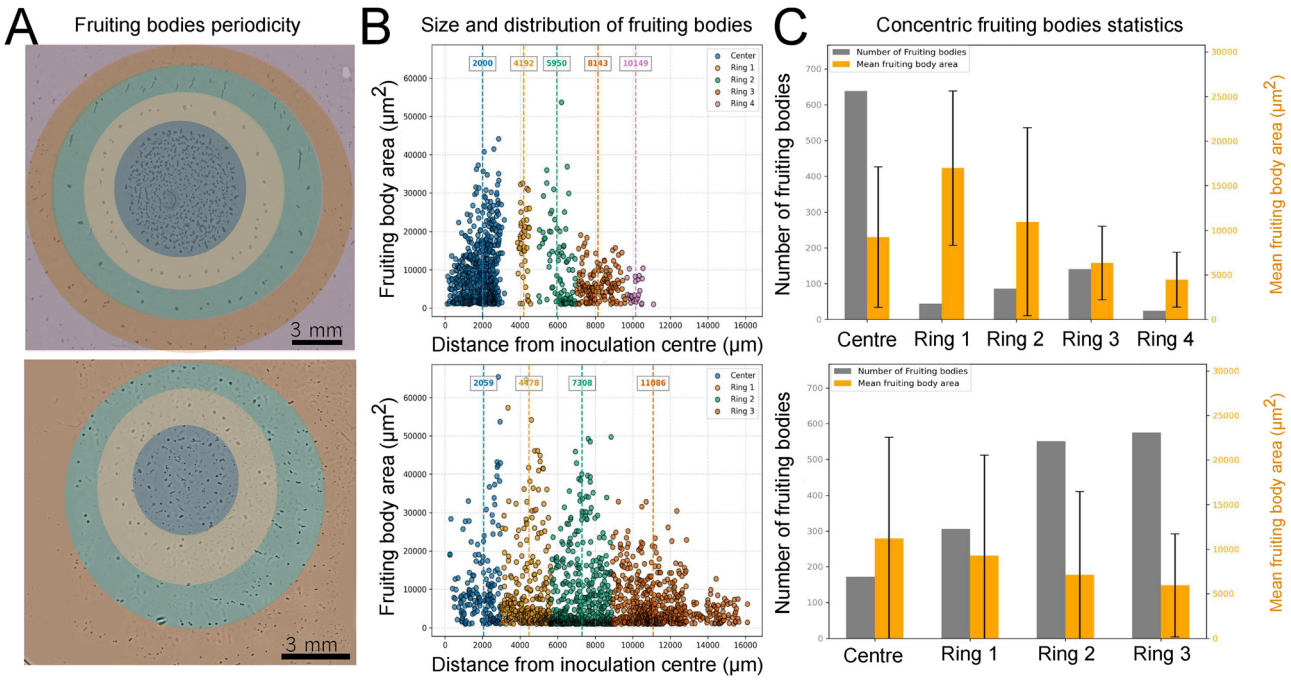

Fig. 6 Analysis of fruiting body patterning by *M. xanthus* after two weeks, comparing a dense population (top row) and a sparse population (bottom row). (A) Visual separation of fruiting bodies in distance intervals from the center of inoculation. (B) Distribution of fruiting body size according to their distance from inoculation site. Where the weighted mean distance, according to area, of each ring is represented by the discontinuous line. (C) Statistical analysis of the fruiting bodies divided by rings. Both the absolute number of fruiting bodies and the mean area of the fruiting body are represented. More replicates are available in the SI for both dense and sparse populations.

produced the highest number of fruiting bodies at the center, though not the largest, while sparse populations generated fewer but comparatively larger structures there. In dense populations, the first ring contained the largest but fewer fruiting bodies, followed by progressively smaller and more numerous ones in outer rings. In sparse populations, this trend was true from the outset, with fruiting bodies decreasing in size and increasing in number across successive rings, although larger structures were rare and ring boundaries less distinct. These results indicate that a threshold cell density is required for the formation of large, well-organized fruiting bodies, whereas smaller, less structured ones emerge under lower-density conditions.

3.3 Predation of other organisms

M. xanthus exhibits predatory behavior through the secretion of antibiotics and hydrolytic enzymes, enabling it to feed on a broad prey range, including Gram-negative[180,181] and Gram-positive bacteria,[182,183] as well as fungi.[184] This behavior is particularly relevant against the rise antibiotic resistance,[79] where some pathogens no longer respond to antibiotic treatments.[185] The use of antibiotics has played a critical role in the overall improvement of society's health conditions but the misuse and improper disposal of antibiotics have led to their presence in wastewater and other environments, promoting resistance through evolutionary pressure by low-dose exposure.[186,187]

To combat antibiotic resistance, researchers are exploring the potential of predatory bacteria like *M. xanthus*.[5] Myxobacteria produce bioactive metabolites in competitive environments,[188] showing effectiveness against multidrug-resistant pathogens. These unique compounds are outperform to standard antibiotics, such as vancomycin, and highlight myxobacteria's vast pharmaceutical potential.[79,180,189] Studying *M. xanthus*'s diverse predatory mechanisms could provide new pathways for drug development.[190]

Active matter interactions can also be investigated through bacterial communities. Processes such as predation, competition, and cooperation[2,191,192] are all observed in *M. xanthus*. Understanding the triggers and rules governing these interactions is of considerable interest in active matter research.[193] Notably, *M. xanthus* exhibits elasticotaxis,[194] providing an alternative to chemotaxis as a mechanism for environmental sensing. *M. xanthus* adapts to different prey and environmental conditions, using a multifactorial approach where digestive enzymes and cell-associated mechanisms play distinct roles. Secreted proteins are more effective against Gram-positive prey, suggesting ecological specialization and complex interactions in microbial communities.[110,195] Additionally, prey organisms may develop "predation resistance" strategies to counter these attacks,[196] as shown in studies identifying resistance genes in *P. aeruginosa* that mitigate *M. xanthus* predation. Resistance mechanisms were related to collateral effects like metal/oxidative stress responses and motility systems[197] stressing the relevance of predation in resistance development.[198]

In this experiment, we use *Escherichia coli* because it is the most widespread bacterial strain used in laboratories. However, using the proper medium and growth conditions, any other microorganism can be used in experiments instead.

Even though predation can be observed in both TPM and CTT media, TPM is preferred to induce starvation and limit the source of nutrition exclusively to the prey.[80] A colony of *M. xanthus* in TPM is not perceptible, but the progressive shrinkage of the limits of prey domain, as shown in Fig. 7A, can be easily seen by naked eye.

In later stages, a waving pattern known as rippling will be formed by *M. xanthus* on the prey colony[199] (see Video S11). Rippling is the result of traveling waves of cells driven by coordinated reversals[200,201] and contact-mediated signaling.[202,203] These oscillations enhance predation efficiency and can be explained by models linking reversal frequency, velocity, and wavelength.[200] Recent work shows that transitions between swarming and rippling depend on local alignment and refractory periods, highlighting polarity-based reversals as a central mechanism of pattern formation.[204,205] The waves interact with each other at the edges of the colony, forming an interference pattern as that shown in Fig. 7B (see Video S12). Pattern formation in active systems remains a key focus of the field,[206] though research often relies on simulations and theoretical frameworks[207,208] rather than experimental studies.[209] The rippling behavior of *M. xanthus* offers a unique opportunity to investigate synchronization among active entities[210] and the emergence of complex interference patterns in physical systems.[211]

After the prey is fully assimilated, high density and starvation conditions are reached, leading to the potential formation of a fruiting body.[9,212] At the cell level, *M. xanthus* cells infiltrate and align along the edge of the colony before rippling starts, as shown in Fig. 7C (see Video S13). Rippling can still be appreciated at the microscopic scale; however the cell density involved to produce rippling phenomena does not allow to distinguish single cells in Fig. 7D (see Video S14), even though it is possible to replicate in a monolayer.[203]

For these experiments, while liquid cultures of *M. xanthus* are being prepared, a Falcon tube containing lysogeny broth is inoculated with the desired prey strain (*E. coli* for this tutorial) under sterile conditions. Grow the prey over 24 hours at the optimal temperature (37 °C) while shaking at 250 rpm.

The prey cells are then pelleted and washed similarly to *M. xanthus*. Take 1 mL of the cultivated prey media at the desired concentration (in this example, 0.5 OD_{600}) and place it in an Eppendorf tube. Centrifuge for 5 minutes at 8000 rpm (approximately 4300*g* relative centrifugal force). In a sterile environment, carefully remove the supernatant, leaving only the pellet at the bottom of the tube.

Add 1 mL of liquid TPM to the pellet and resuspend it using a vortex. Centrifuge again for 5 minutes at 8000 rpm, then carefully remove the supernatant, leaving only the pellet. Add 100 μL (one-tenth of the original suspension volume) of liquid TPM to adjust the concentration. This concentration ensures a dense colony with no spacing between cells, but the prey

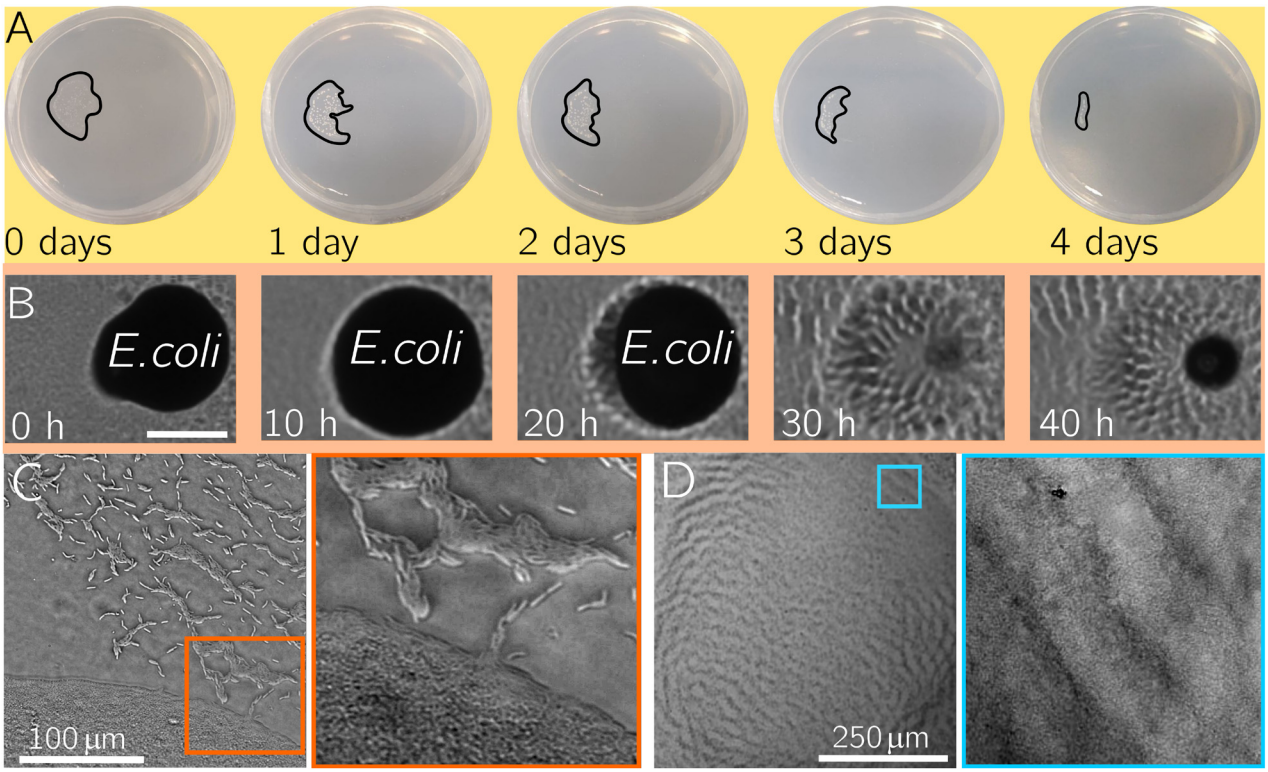

Fig. 7 Predation of *Escherichia coli* by *M. xanthus*. (A) Timelapse of predation on *E. coli* colonies (highlighted by a solid line) by *M. xanthus* with images taken every day since predator/prey contact. The images show the full Petri dish of 55 mm of diameter over a black background to highlight the colonies. (B) Close-up on the progressive predation of a colony during a period of 40 hours since contact with a front of *M. xanthus*. A fruiting body emerged at 40 hours. (C) Microscopic view of the first moment of predator/prey contact before rippling. (D) Fully assimilated colony at 10× objective magnification, where rippling can be observed in the full surface of the colony with a close up at 63× objective magnification.

concentration can be modified to achieve the desired colony density.

Next, place a droplet of 13 μL of *M. xanthus* on the surface of a TPM agar plate. At a distance of approximately 0.5 cm, place a droplet of 5 μL of the prey organism, *E. coli*, ensuring the droplets do not come into contact before drying completely.

Seal the agar plate with its lid using parafilm, and incubate at 32 °C, observing frequently. For macroscopic observations, take images every hour over 72 hours. For microscopic observations, begin imaging once both colonies are almost in contact, capturing images every 2 to 10 minutes over at least 72 hours.

The rippling pattern manifests not only in space but also in time. The analysis was carried out using frames from Video S14, where individual cells appear indistinguishable but the cell density is represented by the intensity of dark and light areas. A dynamic analysis was performed to characterize the periodicity of the rippling wave during predation on *E. coli* in TPM medium solidified with 1.5% agar. The script for the procedure is provided in the SI. The analysis involves extracting the longest line containing relevant information from the video (in this case, the diagonal of Video S14). This line is then plotted over time to generate a time–space representation of the oscillatory behavior, as shown in Fig. 8A. Fast Fourier transform (FFT) is then applied in both the spatial and temporal directions to determine the dominant frequencies corresponding to each magnitude. Different rippling patterns may require different sampling strategies. A higher acquisition frequency than the current 3-minute interval would be necessary to characterize faster rippling phenomena. A sample of the normalized intensity over time (for a single pixel) and space (for a single frame) is also shown in Fig. 8B. Each of these lines, representing either a vertical (time) or horizontal (space) profile, can be analysed using a fast Fourier transform (FFT) to determine the dominant frequencies defining their behavior. All spectra were averaged to obtain the general behavior shown in Fig. 8C. The highest frequency in the temporal domain corresponded to a period of approximately 12 minutes, while the highest spatial frequency corresponded to approximately 54 μm. These values allow for calculation of the rippling wave's propagation speed, which was determined to be 4.5 μm per minute.

3.4 Effect of microparticles

Analysing active matter in complex environments provides crucial insights into how organisms like *M. xanthus* adapt to environmental cues, highlighting the interplay between physical, biochemical, and mechanical factors in microbial behavior. For example, blue light triggers carotenogenesis in *M. xanthus*, demonstrating how environmental stimuli can drive collective cellular responses, which is of great interest in biotechnology.[213] Similarly, the coordinated movement of cells during aggregation and the formation of complex patterns, such as ripples and fruiting bodies, is shaped by external conditions like temperature, substrate stiffness, and aeration.[214–216] Mathematical models, such as Monte Carlo simulations of ripple formation[214] and liquid crystal models of topological defects,[124] are enhanced by incorporating realistic bacterial environments to better understand emergent behaviors under physical constraints. Furthermore, tracking and computational methods show how bacterial motility is modulated by environmental changes, including mechanical forces and nutrient availability, allowing for the simulation of

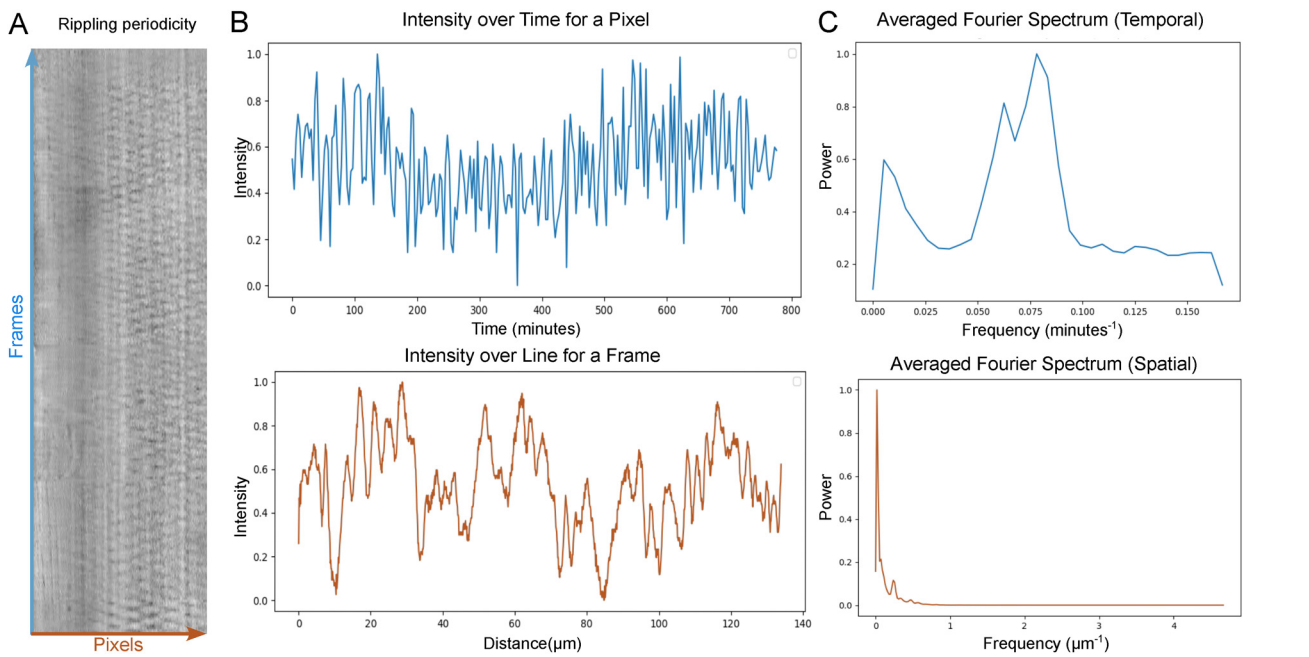

Fig. 8 Analysis of rippling behavior of *M. xanthus*. (A) Visualization of the periodic patterns over time on a sigle line represented on a time-space plane. (B) Intensity distribution over time for a single pixel (upper panel) and along a line in space for a single time point (lower panel). (C) Their corresponding averaged Fourier spectrum. The spectra include all time points, with vertical lines indicating the dominant frequencies at the peaks. The maximum of each spectrum defines the characteristic frequency, whose inverse corresponds to the period in both time and space.

bacterial responses under sparse or stressed conditions.[29,217] These insights are crucial for recreating natural microbial environments and exploring microbial dark matter, revealing previously unobserved behaviors and interactions within diverse ecosystems.[153,195] By integrating more diverse experimental conditions and enriched environments, we can better understand the evolutionary advantages of collective behavior, paving the way for manipulating microbial communities in applications.

Microparticles introduce a level of complexity to the environment that can interfere with the displacement of cells and the emergence of collective behavior. In the case of agar, the deposition of particles can strain the hydrogel structure and in turn be detected by *M. xanthus*. The bacteria are then directed to the source of tension in their movement in a behavior known as elasticotaxis[15,218] (see Video S15).

In this example, adapted from the novel observations from Ramos *et al.*,[13] we use microparticles to alter the environment topography. We use 7 μm diameter melamine resin particles (Microparticles Gmbh, MF-R-8060) (note that different particles might produce different effects). In experiments, bacteria will be drawn to the particles and avoid further organization.[13] As a result, regions with a high concentration of microparticles show almost no visible macroscopic fruiting bodies during the same time frame, while regions with a lower concentration display more fruiting bodies, as illustrated in Fig. 9A. Fruiting bodies can still be observed in the vicinity of the microparticles like in Fig. 9B. At a microscopic level, less spores can be seen in the incipient fruiting body of concentrated substrate while diluted samples still show densely packed fruiting bodies after 96 hours as in Fig. 9C.

An in-depth guide on preparing the agar plate substrates with microparticles can be found in the SI: 2.10 Preparation of substrates with microparticles. Once prepared the substrate with the desired particle concentration, place 13 μL of *M. xanthus* at the center of the region containing the microparticles. For macroscopic observations, take images every hour for a total of 96 hours, comparing results between different particle concentrations. For microscopic observations, capture images every 2 to 20 minutes over the same 96-hour period.

To highlight the impact of microparticles, the resulting fruiting bodies in their absence (Fig. 10A) were compared to those in the concentrated microparticle condition (Fig. 10B). Significantly fewer fruiting bodies formed in the absence of microparticles, with a larger average size, as shown in Fig. 10C. These findings suggest that microparticle obstacles may act as nucleation sites that guide bacterial organization, promoting the emergence of structures typically triggered only at higher cell densities. Consequently, obstacles influence both the spatial distribution and the effective concentration of cells. The presence of microparticles concentrates cells locally in their vicinity while creating a more uniform spread across the surface, leading to an overall lower average cell concentration. This redistribution effect may also contribute to the delayed formation of more numerous yet smaller fruiting bodies.

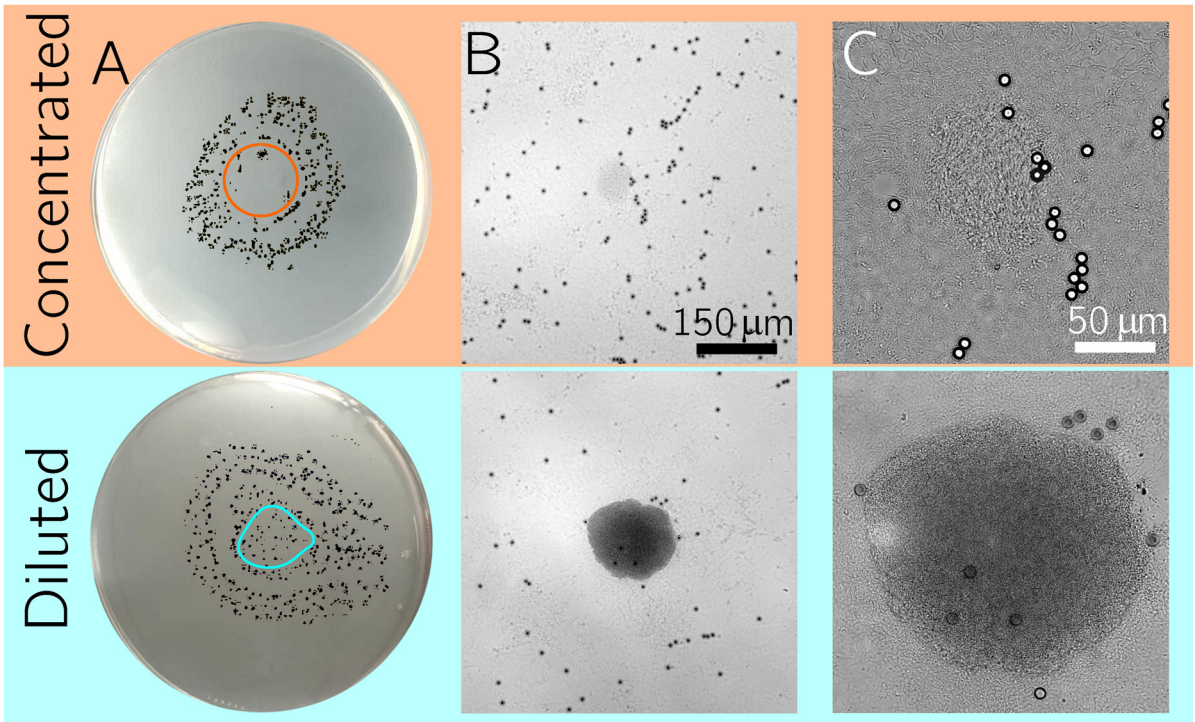

Fig. 9 Effect of microparticles on fruiting body formation. (A) Comparison between substrates deposited with concentrated and diluted microparticles showing the full 55-mm-diameter Petri dish after 96 hours. The area where particles where deposited are circled for each case and the fruiting bodies highlighted in black. (B) Comparison of both substrates at 20× objective magnification showing a fruiting body. (C) Close-up at 63× objective magnification of each previous fruiting body where myxospores and cells can be distinguished.

An alternative approach involves the use of smaller particles transported by bacteria. While bacterial motility is known to enhance diffusion in liquid media,[219–221] *M. xanthus* provides a flat, solid-surface system, opening new avenues for studying particle dynamics and potential applications. Similar setups have been used to study the enhancement of diffusion and transport of passive particles in different experimental conditions, such as bacterial suspensions in a liquid film[222] or in a confined chamber.[223] If inocula are not allowed to dry, surface tension effects, such as the coffee-ring effect,[224–226] can also be explored in combination with active and passive particles.

4 Conclusions

This tutorial provides a comprehensive guide to culturing *M. xanthus*, a bacterial strain with significant potential for active matter studies.[88,174,227–230] While some studies have developed models to explain emergent patterns,[177,231–233] substantial knowledge gaps remain in capturing the multiscale behavior of *M. xanthus* and in validating these models against experimental data. Key areas for further exploration include transitions between behavioral stages, effects of external conditions, and studies in natural or nature-mimicking environments.

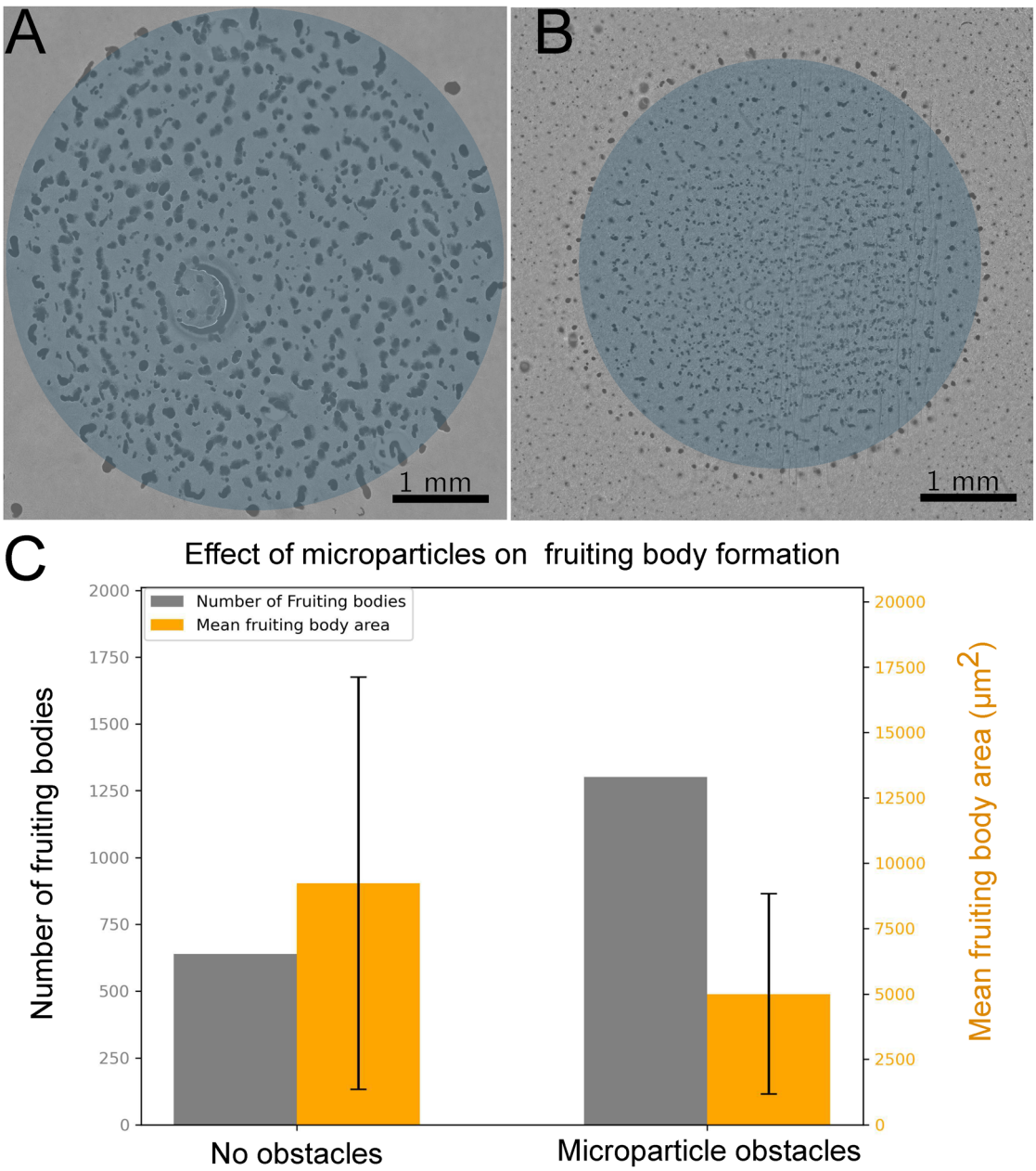

Fig. 10 Quantification of the effect of microparticles on fruiting body formation. Reproducing experiments from Ramos *et al.* 2021[13] (A) fruiting bodies occurring in the inoculation site, highlighted in color, in the absence of microparticles after two weeks. (B) Fruiting bodies occurring in the inoculation site in the presence of a concentrated field of microparticles after two weeks. (C) Statistical data corresponding to the formed fruiting bodies for each case, representing the number of fruiting bodies and their size. More replicates are available for both cases in the SI.

A major challenge in advancing this field has been the entry barrier for researchers without specific microbiological expertise. By lowering this barrier, we aim to promote interdisciplinary research and stimulate further investigation into the promising world of active matter and *M. xanthus*. To this end, we present clear, comprehensive steps for culturing *M. xanthus*, ensuring accessibility even for researchers new to bacterial culture. The reproducibility of these methods has been validated across different researchers and laboratories, reinforcing their reliability. Additionally, we describe simple yet informative experiments that can be performed with *M. xanthus*, studying its behavior at both micro- and macroscopic scales. These include observations of collective movement patterns and social behaviors, providing a solid starting point for more advanced studies.

Bridging the technical gap for researchers from various disciplines to work with *M. xanthus*, this tutorial aims at catalysing innovative active matter research and at offering new insights into bacterial collective behaviors.

Author contributions

Jesus Manuel Antúnez Domínguez: funding acquisition, investigation, methodology, data curation, software, visualization, writing – original draft. Laura Pérez García: funding acquisition, investigation, methodology, data curation, visualization, writing – original draft. Natsuko Rivera-Yoshida: funding acquisition, investigation, methodology, writing – review & editing. Jasmin Di Franco: investigation, validation, writing – review & editing. David Steiner: investigation, validation, writing – review & editing. Alejandro V. Arzola: funding acquisition, resources, supervision, writing – review & editing. Mariana Benítez: funding acquisition, resources, supervision, writing – review & editing. Charlotte Hamngren Blomqvist: resources, validation, writing – review & editing. Roberto Cerbino: funding acquisition, resources, supervision, writing – review & editing. Caroline Beck Adiels: conceptualization, funding acquisition, investigation, methodology, project administration, resources, supervision, writing – review & editing. Giovanni Volpe: conceptualization, funding acquisition, project administration, resources, supervision, writing – review & editing.

Conflicts of interest

There are no conflicts of interest to declare.

Data availability

The data supporting this article have been included as part of the supplementary information (SI) folder within the submission files. The supplementary information includes detailed descriptions of the reagents, materials, equipment, and stock solution recipes used: Reagents and Materials, Stock Solutions & Media. It also provides step-by-step guides for: Media Preparation, From Frozen Stock to Culture, Sample Washing for Experiments, Microparticle Substrate Preparation, and Petri Dish Adaptation for Microscopy. An example of analysis and the extracted data from cell tracking and fruiting body analysis are included: Cell Motility & Tracking, Fruiting Body Analysis, along with the Python scripts used for rippling analysis. Additionally, the supplementary information contains replicates of the quantitative analysis of fruiting bodies formation (and original images) and the supplementary videos: Supplementary Video 1 Development of a *M. xanthus* colony in CTT agar. Supplementary Video 2 Adventurous motility of *M. xanthus* on TPM agar. Supplementary Video 3 Social motility of *M. xanthus* on TPM agar. Supplementary Video 4 Flare formation of *M. xanthus* on TPM agar. Supplementary Video 5 Flare development in a *M. xanthus* colony on CTT agar. Supplementary Video 6 Layer organization of *M. xanthus* colony on TPM agar. Supplementary Video 7 Development of a dense *M. xanthus* colony on TPM agar. Supplementary Video 8 Development of fruiting bodies by *M. xanthus* colony on TPM. Supplementary Video 9 Development of a sparse *M. xanthus* colony on TPM agar. Supplementary Video 10 Fruiting body formation on TPM agar at the microscopic level. Supplementary Video 11 *M. xanthus* predation fronts advancing on *E. coli* colonies. Supplementary Video 12 Edge interactions of *M. xanthus* colonies during predation of *E. coli*. Supplementary Video 13 Microscopic flare formation and infiltration of *E. coli* colonies by *M. xanthus*. Supplementary Video 14 Rippling dynamics and dendritic structure formation at prey edges. Supplementary Video 15 Elasticotaxis of *M. xanthus* on TPM agar due to microparticles. Tracking Video Manual cell tracking performed on supplementary video 4. See DOI: **https://doi.org/10.1039/d5sm00284b**.

Acknowledgements

Jesus Manuel Antunez Dominguez, Caroline Beck Adiels, and Giovanni Volpe acknowledge support from the MSCA-ITN-ETN project ActiveMatter sponsored by the European Commission (Horizon 2020, Project Number 812780). Jesus Manuel Antunez Dominguez and Laura Pérez García Dominguez thank the Adlerbertska forskningsstiftelsen program from years 2022 and 2023 respectively. Natsuko Rivera, Caroline Beck Adiels, and Giovanni Volpe thank the Linnaeus-Palme International Exchange Program. Natsuko Rivera-Yoshida, Mariana Benítez and Alejandro V. Arzola gratefully acknowledge the financial support of the John Templeton Foundation (#62220). Alejandro V. Arzola also acknowledges the financial support of UNAM-DGAPA-PAPIIT (project IN104924) and PASPA-DGAPA. The opinions expressed in this paper are those of the authors and not those of the John Templeton Foundation. Giovanni Volpe acknowledge support from the project ERC-CoG project MAPEI sponsored by the European Commission (Horizon 2020, Project No. 101001267) and from the Knut and Alice Wallenberg Foundation (Grant No. 2019.0079).

Notes and references

1 H. Reichenbach, *Environ. Microbiol.*, 1999, **1**, 15–21.
2 F. J. Contreras-Moreno, J. Pérez, J. Muñoz-Dorado, A. Moraleda-Muñoz and F. J. Marcos-Torres, *Front. Microbiol.*, 2024, **15**, 1339696.

3 T. Clements-Decker, M. Kode, S. Khan and W. Khan, *Front. Chem.*, 2022, 10.
4 S. Saha, S. Sureshkumar, V. Sharma and S. Pande, *npj Antimicrob. Resist.*, 2025, **3**, 49.
5 J. Pérez, F. J. Contreras-Moreno, F. J. Marcos-Torres, A. Moraleda-Muñoz and J. Muñoz-Dorado, *Comput. Struct. Biotechnol. J.*, 2020, **18**, 2547–2555.
6 F. D. Müller, C. W. Schink, E. Hoiczyk, E. Cserti and P. I. Higgs, *Mol. Microbiol.*, 2012, **83**, 486–505.
7 R. B. Nehring, G. Schisler, L. Chiaramonte, A. Horton and B. Poole, *J. Aquat. Anim. Health*, 2015, **27**, 50–56.
8 D. Lall, M. M. Glaser and P. I. Higgs, *Appl. Environ. Microbiol.*, 2024, **90**(10), e0166024.
9 J. E. Berleman and J. R. Kirby, *J. Bacteriol.*, 2007, **189**, 5675–5682.
10 D. Claessen, D. E. Rozen, O. P. Kuipers, L. Søgaard-Andersen and G. P. van Wezel, *Nat. Rev. Microbiol.*, 2014, **12**, 115–124.
11 R. Mercier and T. Mignot, *Curr. Opin. Microbiol.*, 2016, **34**, 104–110.
12 J. A. A. D. Angel, V. Nanjundiah, M. Benítez and S. A. Newman, *EvoDevo*, 2020, **11**, 21.
13 C. H. Ramos, E. Rodríguez-Sánchez, J. A. A. D. Angel, A. V. Arzola, M. Benítez, A. E. Escalante, A. Franci, G. Volpe and N. Rivera-Yoshida, *Sci. Adv.*, 2021, **7**(35), eabh2278.
14 G. R. Janssen, J. W. Wireman and M. Dworkin, *J. Bacteriol.*, 1977, **130**, 561–562.
15 M. Dworkin, K. H. Keller and D. Weisberg, *J. Bacteriol.*, 1983, **155**, 1367–1371.
16 J. Starruß, F. Peruani, V. Jakovljevic, L. Søgaard-Andersen, A. Deutsch and M. Bär, *Interface Focus*, 2012, **2**, 774–785.
17 N. Rivera-Yoshida, A. V. Arzola, J. A. A. D. Angel, A. Franci, M. Travisano, A. E. Escalante and M. Benítez, *R. Soc. Open Sci.*, 2019, **6**, 181730.
18 C. Bechinger, R. Di Leonardo, H. Löwen, C. Reichhardt, G. Volpe and G. Volpe, *Rev. Mod. Phys.*, 2016, **88**, 045006.
19 O. Hallatschek, S. S. Datta, K. Drescher, J. Dunkel, J. Elgeti, B. Waclaw and N. S. Wingreen, *Nat. Rev. Phys.*, 2023, **5**, 407–419.
20 A. J. Mathijssen, *Biophys. J.*, 2024, **123**, 541a.
21 J. G. Mitchell and K. Kogure, *FEMS Microbiol. Ecol.*, 2006, **55**, 3–16.
22 N. Wadhwa and H. C. Berg, *Nat. Rev. Microbiol.*, 2022, **20**, 161–173.
23 C. M. Waters and B. L. Bassler, *Annu. Rev. Cell Dev. Biol.*, 2005, **21**, 319–346.
24 O. P. Duddy and B. L. Bassler, *PLoS Pathog.*, 2021, **17**, e1009074.
25 A. Shrestha, M. Grimm, I. Ojiro, J. Krumwiede and A. Schikora, *Front. Microbiol.*, 2020, 11.
26 B. Nasslahsen, Y. Prin, H. Ferhout, A. Smouni and R. Duponnois, *Front. Soil Sci.*, 2022, 2.
27 L. Wu and Y. Luo, *Front. Microbiol.*, 2021, **12**, 611413.
28 G. Coquant, D. Aguanno, S. Pham, N. Grellier, S. Thenet, V. Carrière, J.-P. Grill and P. Seksik, *World J. Gastroenterol.*, 2021, **27**, 7247–7270.
29 N. Rivera-Yoshida, A. V. Arzola and M. Benítez, *Biol. Lett.*, 2024, **20**(10), 20240360.
30 A. Be'er, B. Ilkanaiv, R. Gross, D. B. Kearns, S. Heidenreich, M. Bär and G. Ariel, *Commun. Phys.*, 2020, **3**, 66.
31 J. D. Partridge, *Surveying a Swarm: Experimental Techniques To Establish and Examine Bacterial Collective Motion*, 2022.
32 C. Zhang and B. K. Hammer, *Curr. Biol.*, 2023, **33**, R1063–R1064.
33 J. Pan, J. Zhou, X. Tang, Y. Guo, Y. Zhao and S. Liu, *Environ. Sci. Technol.*, 2023, **57**, 4253–4265.
34 I. Grobas, M. Polin and M. Asally, *eLife*, 2021, **10**, e62632.
35 J. D. Partridge and R. M. Harshey, *J. Bacteriol.*, 2013, **195**, 909–918.
36 J. D. Partridge, N. T. Q. Nhu, Y. S. Dufour and R. M. Harshey, *mBio*, 2019, **10**(2), e00316-19.
37 P. de Castro, S. Diles, R. Soto and P. Sollich, *Soft Matter*, 2021, **17**, 2050–2061.
38 S. Kamdar, S. Shin, P. Leishangthem, L. F. Francis, X. Xu and X. Cheng, *Nature*, 2022, **603**, 819–823.
39 E. Lushi, H. Wioland and R. E. Goldstein, *Proc. Natl. Acad. Sci. U. S. A.*, 2014, **111**, 9733–9738.
40 C. W. Wolgemuth, *Biophys. J.*, 2008, **95**, 1564–1574.
41 J. Gachelin, A. Rousselet, A. Lindner and E. Clement, *New J. Phys.*, 2014, **16**, 025003.
42 D. L. Koch and G. Subramanian, *Annu. Rev. Fluid Mech.*, 2011, **43**, 637–659.
43 G. C. Padron, A. M. Shuppara, J.-J. S. Palalay, A. Sharma and J. E. Sanfilippo, *J. Bacteriol.*, 2023, 205.
44 I. S. Aranson, *Rep. Prog. Phys.*, 2022, **85**, 076601.
45 H. Ueda, K. Stephens, K. Trivisa and W. E. Bentley, *mBio*, 2019, **10**, e00972-19.
46 I. C. Engelhardt, D. Patko, Y. Liu, M. Mimault, G. de las Heras Martinez, T. S. George, M. MacDonald, M. Ptashnyk, T. Sukhodub, N. R. Stanley-Wall, N. Holden, T. J. Daniell and L. X. Dupuy, *ISME J.*, 2022, **16**, 2337–2347.
47 M. M. Abdulkadieva, E. V. Sysolyatina, E. V. Vasilieva, A. I. Gusarov, P. A. Domnin, D. A. Slonova, Y. M. Stanishevskiy, M. M. Vasiliev, O. F. Petrov and S. A. Ermolaeva, *Sci. Rep.*, 2022, **12**, 614.
48 R. M. Losick, *Curr. Biol.*, 2020, **30**, R1146–R1150.
49 M. Krajnc, P. Stefanic, R. Kostanjšek, I. Mandic-Mulec, I. Dogsa and D. Stopar, *npj Biofilms Microbiomes*, 2022, **8**, 25.
50 J. Deng, M. Molaei, N. G. Chisholm and K. J. Stebe, *Langmuir*, 2020, **36**, 6888–6902.
51 S. Gomez, L. Bureau, K. John, E.-N. Chêne, D. Débarre and S. Lecuyer, *eLife*, 2023, **12**, e81112.
52 Y.-R. Chang, E. R. Weeks, D. Barton, J. Dobnikar and W. A. Ducker, *ACS Biomater. Sci. Eng.*, 2019, **5**, 6436–6445.
53 X. Zheng, E. J. Gomez-Rivas, S. I. Lamont, K. Daneshjoo, A. Shieh, D. J. Wozniak and M. R. Parsek, *Proc. Natl. Acad. Sci. U. S. A.*, 2024, **121**, e2411981121.
54 A. M. Spagnolo, M. Sartini and M. L. Cristina, *Rev. Med. Microbiol.*, 2021, **32**, 169–175.
55 A. Yang, W. S. Tang, T. Si and J. X. Tang, *Biophys. J.*, 2017, **112**, 1462–1471.
56 H. Wang, F. Li, L. Xu, H. Byun, J. Fan, M. Wang, M. Li, J. Zhu and B. Li, *Appl. Environ. Microbiol.*, 2021, **87**, e00938-21.

57 A. Frederick, Y. Huang, M. Pu and D. A. Rowe-Magnus, *J. Bacteriol.*, 2020, **202**, e00261-20.
58 R. C. V. Coelho, N. A. M. Araújo and M. M. T. da Gama, *Soft Matter*, 2020, **16**, 4256–4266.
59 C. Fylling, J. Tamayo, A. Gopinath and M. Theillard, *Soft Matter*, 2024, **20**, 1392–1409.
60 G. Prado, E. T. Mendes, R. C. R. Martins, L. V. Perdigão-Neto, M. P. Freire, A. P. Marchi, M. F. Côrtes, V. A. C. de Castro Lima, F. Rossi, T. Guimarães, A. S. Levin and S. F. Costa, *Int. J. Antimicrob. Agents*, 2022, **59**, 106463.
61 M. S. Mulani, E. E. Kamble, S. N. Kumkar, M. S. Tawre and K. R. Pardesi, *Front. Microbiol.*, 2019, **10**, 539.
62 R. Jose and V. Singh, *J. Indian Inst. Sci.*, 2020, **100**, 515–524.
63 L. Kroos, D. Wall, S. T. Islam, D. E. Whitworth, J. Muñoz-Dorado, P. I. Higgs, M. Singer, E. M. Mauriello, A. Treuner-Lange, L. Søgaard-Andersen, C. Kaimer, M. Elías-Arnanz, E. A. Stojković, R. Müller, C. Volz, G. J. Velicer and B. Nan, *J. Bacteriol.*, 2025, **207**(7), e00071-25.
64 E. M. F. Mauriello, T. Mignot, Z. Yang and D. R. Zusman, *Microbiol. Mol. Biol. Rev.*, 2010, **74**, 229–249.
65 D. B. Kearns, *Nat. Rev. Microbiol.*, 2010, **8**, 634–644.
66 J. E. Patrick and D. B. Kearns, *Mol. Microbiol.*, 2012, **83**, 14–23.
67 M. Burkart, A. Toguchi and R. M. Harshey, *Proc. Natl. Acad. Sci. U. S. A.*, 1998, **95**, 2568–2573.
68 S. Mariconda, Q. Wang and R. M. Harshey, *Mol. Microbiol.*, 2006, **60**, 1590–1602.
69 K. Hamze, S. Autret, K. Hinc, S. Laalami, D. Julkowska, R. Briandet, M. Renault, C. Absalon, I. B. Holland, H. Putzer and S. J. Séror, *Microbiology*, 2011, **157**, 2456–2469.
70 R. M. Harshey, *Annu. Rev. Microbiol.*, 2003, **57**, 249–273.
71 W. Shi and D. R. Zusman, *Proc. Natl. Acad. Sci. U. S. A.*, 1993, **90**, 3378–3382.
72 A. M. Spormann, *Microbiol. Mol. Biol. Rev.*, 1999, **63**, 621–641.
73 R. M. Behmlander and M. Dworkin, *J. Bacteriol.*, 1994, **176**, 6295–6303.
74 S.-H. Kim, S. Ramaswamy and J. Downard, *J. Bacteriol.*, 1999, **181**, 1496–1507.
75 Y. Wang, T. Li, W. Xue, Y. Zheng, Y. Wang, N. Zhang, Y. Zhao, J. Wang, Y. Li, C. Wang and W. Hu, *Front. Microbiol.*, 2022, **13**, 861865.
76 P. D. Curtis, J. Atwood, R. Orlando and L. J. Shimkets, *J. Bacteriol.*, 2007, **189**, 7634–7642.
77 A. Konovalova, T. Petters and L. Søgaard-Andersen, *FEMS Microbiol. Rev.*, 2010, **34**, 89–106.
78 K. J. Dye, S. Salar, U. Allen, W. Smith and Z. Yang, *J. Bacteriol.*, 2023, **205**(9), e00221-23.
79 B. S. Arakal, R. S. Rowlands, S. E. Maddocks, D. E. Whitworth, P. E. James and P. G. Livingstone, *J. Appl. Microbiol.*, 2025, **136**(1), lxae315.
80 K. L. Hillesland, R. E. Lenski and G. J. Velicer, *Microb. Ecol.*, 2007, **53**, 571–578.
81 S. Müller, S. N. Strack, S. E. Ryan, M. Shawgo, A. Walling, S. Harris, C. Chambers, J. Boddicker and J. R. Kirby, *J. Bacteriol.*, 2016, **198**, 3335–3344.
82 J. E. Berleman, J. Scott, T. Chumley and J. R. Kirby, *Proc. Natl. Acad. Sci. U. S. A.*, 2008, **105**, 17127–17132.
83 J. W. Wireman and M. Dworkin, *J. Bacteriol.*, 1977, **129**, 798–802.
84 P. Cao, A. Dey, C. N. Vassallo and D. Wall, *J. Mol. Biol.*, 2015, **427**, 3709–3721.
85 S. Thutupalli, M. Sun, F. Bunyak, K. Palaniappan and J. W. Shaevitz, *J. R. Soc., Interface*, 2015, **12**(109), 20150049.
86 A. Martínez-Laborda, J. M. Balsalobre, M. Fontes and F. J. Murillo, *Mol. Gen. Genet.*, 1990, **223**, 205–210.
87 R. Pérez-Castaño, E. Bastida-Martínez, J. Fernández-Zapata, M. del Carmen Polanco, M. L. Galbis-Martínez, A. A. Iniesta, M. Fontes, S. Padmanabhan and M. Elías-Arnanz, *Environ. Microbiol.*, 2022, **24**, 1865–1886.
88 C. R. Cotter, H.-B. Schüttler, O. A. Igoshin and L. J. Shimkets, *Proc. Natl. Acad. Sci. U. S. A.*, 2017, **114**, E4592–E4601.
89 G. Liu, A. Patch, F. Bahar, D. Yllanes, R. D. Welch, M. C. Marchetti, S. Thutupalli and J. W. Shaevitz, *Phys. Rev. Lett.*, 2019, **122**, 248102.
90 G. J. Velicer and Y. T. N. Yu, *Nature*, 2003, **425**, 75–78.
91 H. Zhang, S. Angus, M. Tran, C. Xie, O. A. Igoshin and R. D. Welch, *J. Bacteriol.*, 2011, **193**, 5164–5170.
92 M. Peleg and M. G. Corradini, *Crit. Rev. Food Sci. Nutr.*, 2011, **51**, 917–945.
93 Y. J. Yang, R. P. Singh, X. Lan, C. S. Zhang, D. H. Sheng and Y. Q. Li, *Microb. Cell Fact.*, 2019, **18**, 123.
94 Z. Pan, Z. Zhang, L. Zhuo, T. Y. Wan and Y. Z. Li, *mSphere*, 2021, **6**, e00305-21.
95 T. Wan, Y. Cao, Y. J. Lai, Z. Pan, Y. Z. Li and L. Zhuo, *mSphere*, 2024, **9**(9), e00363-24.
96 W. Hu, Y. Wang, X. Yue, W. Xue, W. Hu, X. Yue and Y. Li, *Eng. Microbiol.*, 2024, **4**, 100155.
97 R. Tennant and P. Rutten, *Calibration Protocol – Conversion of OD600 to Colony Forming Units (CFUs) v1*, 2019.
98 A. C. Ogodo, D. I. Agwaranze, M. Daji and R. E. Aso, *Microbial techniques and methods: basic techniques and microscopy*, Elsevier, 2022, pp. 201–220.
99 B. Houchmandzadeh and P. Ballet, *J. Microbiol. Methods*, 2023, **206**, 106693.
100 W. Dawid, *FEMS Microbiol. Rev.*, 2000, **24**, 403–427.
101 J. P. Karwowski, G. N. Sunga, S. Kadam and J. B. McAlpine, *J. Ind. Microbiol.*, 1996, **16**, 230–236.
102 Z. Vaksman and H. B. Kaplan, *Curr. Protoc. Microbiol.*, 2015, **39**, 7A.1.1–7A.1.21.
103 L. Ta, L. Gosa and D. A. Nathanson, *Biosafety and Biohazards: Understanding Biosafety Levels and Meeting Safety Requirements of a Biobank*, Humana Press Inc., 2019, vol. 1897, pp. 213–225.
104 C. E. Morrison and D. R. Zusman, *J. Bacteriol.*, 1979, 1036–1042.
105 S. L. Morrison, *Curr. Protoc. Immunol.*, 1997, **21**(1), A.3M.
106 R. G. Taylor and R. D. Welch, *J. Visualized Exp.*, 2010, **42**, e2038.
107 I. G. de Jong, K. Beilharz, O. P. Kuipers and J.-W. Veening, *J. Visualized Exp.*, 2011, **53**, 3145.

108 W. Hu, L. Li, S. Sharma, J. Wang, I. McHardy, R. Lux, Z. Yang, X. He, J. K. Gimzewski, Y. Li and W. Shi, *PLoS One*, 2012, **7**, e51905.
109 W. P. Black and Z. Yang, *J. Bacteriol.*, 2004, **186**, 1001–1008.
110 K. I. Arend, J. J. Schmidt, T. Bentler, C. Lüchtefeld, D. Eggerichs, H. M. Hexamer and C. Kaimer, *Appl. Environ. Microbiol.*, 2021, **87**, 1–17.
111 R. Lux, Y. Li, A. Lu and W. Shi, *Biofilms*, 2004, **1**, 293–303.
112 J. Wang, W. Hu, R. Lux, X. He, Y. Li and W. Shi, *J. Bacteriol.*, 2011, **193**, 2122–2132.
113 D. Schumacher and L. Søgaard-Andersen, *J. Visualized Exp.*, 2018, 2018.
114 A. Ducret, B. Fleuchot, P. Bergam and T. Mignot, *eLife*, 2013, 2013.
115 J. Zhang, J. A. Comstock, C. R. Cotter, P. A. Murphy, W. Nie, R. D. Welch, A. B. Patel and O. A. Igoshin, *Microorganisms*, 2021, **9**(9), 1954.
116 L. M. Alexander and J.-P. van Pijkeren, *Trends Microbiol.*, 2023, **31**, 197–211.
117 S. N. Gómez-Barrera, W. Ángel Delgado-Tapia, A. E. Hernández-Gutiérrez, M. Cayetano-Cruz, C. Méndez and I. Bustos-Jaimes, *ACS Omega*, 2025, **10**, 7142–7152.
118 Y.-S. Lin, M.-Y. Lee, C.-H. Yang and K.-S. Huang, *Curr. Top. Med. Chem.*, 2015, **15**, 1525–1531.
119 A. Doostmohammadi, J. Ignés-Mullol, J. M. Yeomans and F. Sagués, *Nat. Commun.*, 2018, **9**, 3246.
120 A. Sengupta, *Front. Phys.*, 2020, **8**, 184.
121 J. Nijjer, C. Li, M. Kothari, T. Henzel, Q. Zhang, J.-S. B. Tai, S. Zhou, T. Cohen, S. Zhang and J. Yan, *Nat. Phys.*, 2023, **19**, 1936–1944.
122 Y. I. Yaman, E. Demir, R. Vetter and A. Kocabas, *Nat. Commun.*, 2019, **10**, 2285.
123 D. Dell'Arciprete, M. L. Blow, A. T. Brown, F. D. C. Farrell, J. S. Lintuvuori, A. F. McVey, D. Marenduzzo and W. C. K. Poon, *Nat. Commun.*, 2018, **9**, 4190.
124 K. Copenhagen, R. Alert, N. S. Wingreen and J. W. Shaevitz, *Nat. Phys.*, 2021, **17**, 211–215.
125 M. Sourice, C. Simmler, M. Maresca, B. Py and C. Aubert, *Microbiol. Spectrum*, 2024, **12**(12), e01740-24.
126 L. Zhang, L. Guo, Z. Cui and F. Ju, *Trends Microbiol.*, 2024, **32**, 398–409.
127 A. N. Yadav, D. Kour and N. Yadav, *J. Appl. Biol. Biotechnol.*, 2024, **12**, i–iii.
128 S. Saha, D. Paul, T. R. Poudel, N. M. Basunia, T. Hasan, M. Hasan, B. Li, R. Reza, A. R. Haque, M. A. Hanif, M. Sarker, N. J. Roberts, M. A. Khoso, H. Wu and H. L. Shen, *J. Appl. Biol. Biotechnol.*, 2023, **11**, 31–44.
129 L. Zhang, L. Bao, S. Li, Y. Liu and H. Liu, *Front. Microbiol.*, 2024, **14**, 1294854.
130 S. T. Islam, I. V. Alvarez, F. Saïdi, A. Guiseppi, E. Vinogradov, G. Sharma, L. Espinosa, C. Morrone, G. Brasseur, J.-F. Guillemot, A. Benarouche, J.-L. Bridot, G. Ravicoularamin, A. Cagna, C. Gauthier, M. Singer, H.-P. Fierobe, T. Mignot and E. M. F. Mauriello, *PLoS Biol.*, 2020, **18**, e3000728.
131 A. P. Karlapudi, T. Venkateswarulu, J. Tammineedi, L. Kanumuri, B. K. Ravuru, V. R. Dirisala and V. P. Kodali, *Petroleum*, 2018, **4**, 241–249.
132 M. Cho, S. Park, E. You and C. Kim, *Geosyst. Eng.*, 2021, **24**, 180–187.
133 J. Pérez, J. Muñoz-Dorado and A. Moraleda-Muñoz, *Metallomics*, 2018, **10**, 876–886.
134 M. L. Merroun, E. Alonso and N. Ben Omar, *Geomicrobiol. J.*, 2001, **18**, 183–192.
135 C. Jimenez-Lopez, F. Jroundi, M. Rodríguez-Gallego and J. Arias, *Communicating current research and educational topics and trends in applied microbiology*, Formatex, 2007, vol. 1, pp. 143–154.
136 M. T. González-Muñoz, C. Rodriguez-Navarro, F. Martínez-Ruiz, J. M. Arias, M. L. Merroun and M. Rodriguez-Gallego, Geological Society, London, Special Publications, 2010, vol. 336, pp. 31–50.
137 C. Rodriguez-Navarro, M. Rodriguez-Gallego, K. B. Chekroun and M. T. Gonzalez-Munoz, *Appl. Environ. Microbiol.*, 2003, **69**, 2182–2193.
138 S. Kataki and D. C. Baruah, *Prospects and Issues of Phosphorus Recovery as Struvite from Waste Streams*, Springer International Publishing, 2019, pp. 821–868.
139 C. L. Hueschen, L. A. Segev-Zarko, J. H. Chen, M. A. LeGros, C. A. Larabell, J. C. Boothroyd, R. Phillips and A. R. Dunn, *Nat. Phys.*, 2024, **20**, 1989–1996.
140 G. L. Miño, M. A. R. Koehl, N. King and R. Stocker, *Limnol. Oceanogr. Lett.*, 2017, **2**, 37–46.
141 C. E. Stanley, G. Grossmann, X. C. Solvas and A. J. DeMello, *Lab Chip*, 2016, **16**, 228–241.
142 C. Arellano-Caicedo, P. Ohlsson, M. Bengtsson, J. P. Beech and E. C. Hammer, *Curr. Biol.*, 2023, **33**, 1448–1458.e4.
143 M. P. Monteiro, J. P. Carrillo-Mora, N. Gutiérrez, S. Montagna, A. R. Lodeiro, M. L. Cordero and V. I. Marconi, *Commun. Biol.*, 2025, **8**(1), 662.
144 L. Solden, K. Lloyd and K. Wrighton, *Curr. Opin. Microbiol.*, 2016, **31**, 217–226.
145 J.-Y. Jiao, L. Liu, Z.-S. Hua, B.-Z. Fang, E.-M. Zhou, N. Salam, B. P. Hedlund and W.-J. Li, *Natl. Sci. Rev.*, 2021, **8**(3), nwaa280.
146 Z. Asghar, N. Ali, O. A. Bég and T. Javed, *Results Phys.*, 2018, **9**, 682–691.
147 Z. Asghar, N. Ali and M. Sajid, *Math. Biosci.*, 2017, **290**, 31–40.
148 R. A. Shah, Z. Asghar and N. Ali, *Eur. Phys. J. Plus*, 2022, **137**, 600.
149 P. Meiser, H. B. Bode and R. Müller, *Proc. Natl. Acad. Sci. U. S. A.*, 2006, **103**, 19128–19133.
150 P. Meiser, K. J. Weissman, H. B. Bode, D. Krug, J. S. Dickschat, A. Sandmann and R. Müller, *Chem. Biol.*, 2008, **15**, 771–781.
151 C. Dinet and T. Mignot, *FEBS Lett.*, 2023, **597**, 850–864.
152 A. L. Koch, *Crit. Rev. Microbiol.*, 2006, **32**, 87–90.
153 L. J. Ritchie, E. R. Curtis, K. A. Murphy and R. D. Welch, *J. Bacteriol.*, 2021, 203.
154 P. Patra, K. Kissoon, I. Cornejo, H. B. Kaplan and O. A. Igoshin, *PLoS Comput. Biol.*, 2016, **12**, e1005010.
155 N. Faiza, R. Welch and A. Patteson, *APL Bioeng.*, 2025, **9**(1), 016104.

156 A. C. Ramírez, K. S. Lee, A. Odriozola, M. Kaminek, R. Stocker, B. Zuber and P. Junier, *Microbiology*, 2023, 169.
157 D. J. Bretl and J. R. Kirby, *J. Mol. Biol.*, 2016, **428**, 3805–3830.
158 J. Muñoz-Dorado, F. J. Marcos-Torres, E. García-Bravo, A. Moraleda-Muñoz and J. Pérez, *Front. Microbiol.*, 2016, **7**, 781.
159 Y. Kimura, S. Kawasaki, H. Yoshimoto and K. Takegawa, *J. Bacteriol.*, 2010, **192**, 1467–1470.
160 F. D. Müller, C. W. Schink, E. Hoiczyk, E. Cserti and P. I. Higgs, *Mol. Microbiol.*, 2012, **83**, 486–505.
161 K. Yoshio, Y. Yoshioka and K. Toshikuni, *J. Microbiol.*, 2022, **60**, 1168–1177.
162 D. Harita, H. Matsukawa and Y. Kimura, *Curr. Microbiol.*, 2024, **81**, 248.
163 H. Do, C. S. Madukoma, V. Sundaresan, J. D. Shrout, A. J. Hoffman and P. W. Bohn, *Anal. Bioanal. Chem.*, 2022, **414**, 1691–1698.
164 Y. Peng, Z. Liu and X. Cheng, *Sci. Adv.*, 2021, 7(17), eabd1240.
165 X. Wang, R. Blumenfeld, X.-Q. Feng and D. A. Weitz, *Phys. Life Rev.*, 2022, **43**, 98–138.
166 J. Y. Wakano, A. Komoto and Y. Yamaguchi, *Phys. Rev. E: Stat., Nonlinear, Soft Matter Phys.*, 2004, **69**, 051904.
167 T. Markovich and T. C. Lubensky, *Phys. Rev. Lett.*, 2021, **127**, 048001.
168 S. Liu, S. Shankar, M. C. Marchetti and Y. Wu, *Nature*, 2021, **590**, 80–84.
169 D. Lall, M. M. Glaser and P. I. Higgs, *Appl. Environ. Microbiol.*, 2024, **90**(10), e01660-24.
170 D. L. Whitfield, G. Sharma, G. T. Smaldone and M. Singer, *Genomics*, 2020, **112**, 1588–1597.
171 S. Pande, P. P. Escriva, Y. T. N. Yu, U. Sauer and G. J. Velicer, *Curr. Biol.*, 2020, **30**, 4745–4752.e4.
172 M. R. Parsek and E. Greenberg, *Trends Microbiol.*, 2005, **13**, 27–33.
173 R. C. MacLean, *Heredity*, 2008, **100**, 233–239.
174 P. Murphy, J. Comstock, T. Khan, J. Zhang, R. Welch and O. A. Igoshin, *mSystems*, 2023, **8**(5), e00425-23.
175 D. Kaiser and R. Welch, *J. Bacteriol.*, 2004, **186**, 919–927.
176 L. Jelsbak and L. Søgaard-Andersen, *Proc. Natl. Acad. Sci. U. S. A.*, 1999, **96**, 5031–5036.
177 O. Sozinova, Y. Jiang, D. Kaiser and M. Alber, *Proc. Natl. Acad. Sci. U. S. A.*, 2006, **103**, 17255–17259.
178 K. A. O'Connor and D. R. Zusman, *J. Bacteriol.*, 1988, **170**, 4103–4112.
179 K. B. Graniczkowska, D. Bizhga, M. Noda, V. Leon, N. Saraf, D. Feliz, G. Sharma, A. C. Nugent, M. Singer and E. A. Stojković, *Photochem. Photobiol. Sci.*, 2024, **23**, 1857–1870.
180 A. D. Morgan, R. C. MacLean, K. L. Hillesland and G. J. Velicer, *Appl. Environ. Microbiol.*, 2010, **76**, 6920–6927.
181 S. Thiery and C. Kaimer, *Front. Microbiol.*, 2020, **11**(2), DOI: 10.3389/fmicb.2020.00002.
182 S. Müller, S. N. Strack, S. E. Ryan, M. Shawgo, A. Walling, S. Harris, C. Chambers, J. Boddicker and J. R. Kirby, *J. Bacteriol.*, 2016, **198**, 3335–3344.
183 D. G. Lloyd and D. E. Whitworth, *Front. Microbiol.*, 2017, **8**, 439.
184 V. Groß, A. Reinhard, S. Petters, M. Pichler and T. Urich, *Eur. J. Soil Biol.*, 2023, **117**, 103508.
185 N. A. Church and J. L. McKillip, *Biologia*, 2021, **76**, 1535–1550.
186 J. Bengtsson-Palme, E. Kristiansson and D. G. J. Larsson, *FEMS Microbiol. Rev.*, 2018, **42**, 68–80.
187 H. Brüssow, *Microb. Biotechnol.*, 2024, **17**, e14510.
188 J. Herrmann, A. A. Fayad and R. Müller, *Nat. Prod. Rep.*, 2017, **34**, 135–160.
189 F. Saadatpour and F. Mohammadipanah, *Folia Microbiol.*, 2020, **65**, 639–648.
190 S. K. Saggu, A. Nath and S. Kumar, *Res. Microbiol.*, 2023, **174**, 104079.
191 M. Gerhard, A. Jayaram, A. Fischer and T. Speck, *Phys. Rev. E*, 2021, **104**, 054614.
192 C.-J. Chen and C. Bechinger, *New J. Phys.*, 2022, **24**, 033001.
193 H. Löwen and B. Liebchen, Towards intelligent active particles, in *Artificial Intelligence and Intelligent Matter*, ed. M. te Vrugt, Springer, Cham, 2025.
194 A. Sengupta, T. Kruppa and H. Löwen, *Phys. Rev. E: Stat., Nonlinear, Soft Matter Phys.*, 2011, **83**, 031914.
195 Z. Zhang, C. R. Cotter, Z. Lyu, L. J. Shimkets and O. A. Igoshin, *mSystems*, 2020, **5**(4), 10-1128.
196 J. Herrou, D. Murat and T. Mignot, *Curr. Opin. Microbiol.*, 2024, **80**, 102492.
197 N. Sydney, M. T. Swain, J. M. So, E. Hoiczyk, N. P. Tucker and D. E. Whitworth, *Microb. Physiol.*, 2021, **31**, 57–66.
198 Z. Wang, Q. Chen, J. Zhang, H. Xu, L. Miao, T. Zhang, D. Liu, Q. Zhu, H. Yan and D. Yan, *Water Res.*, 2024, **256**, 121642.
199 J. E. Berleman, T. Chumley, P. Cheung and J. R. Kirby, *J. Bacteriol.*, 2006, **188**, 5888–5895.
200 H. Zhang, Z. Vaksman, D. B. Litwin, P. Shi, H. B. Kaplan and O. A. Igoshin, *PLoS Comput. Biol.*, 2012, **8**, e1002715.
201 L. L. Bonilla, A. Glavan and A. Marquina, *Phys. Rev. E*, 2016, **93**, 012412.
202 R. Welch and D. Kaiser, *Proc. Natl. Acad. Sci. U. S. A.*, 2001, **98**, 14907–14912.
203 O. Sliusarenko, J. Neu, D. R. Zusman and G. Oster, *Proc. Natl. Acad. Sci. U. S. A.*, 2006, **103**, 1534–1539.
204 J.-B. Saulnier, M. Romanos, J. Schrohe, C. Cuzin, V. Calvez and T. Mignot, *The mechanism of spatial pattern transition in motile bacterial collectives*, 2024.
205 H. Bloch, V. Calvez, B. Gaudeul, L. Gouarin, A. Lefebvre-Lepot, T. Mignot, M. Romanos and J.-B. Saulnier, ESAIM*: Proceedings and Surveys*, 2024, vol. 77, pp. 25–45.
206 G. Volpe, C. Bechinger, F. Cichos, R. Golestanian, H. Löwen, M. Sperl and G. Volpe, *npj Microgravity*, 2022, **8**, 54.
207 D. Vahabli and T. Vicsek, *Commun. Phys.*, 2023, **6**, 56.
208 Y. Zhang and É. Fodor, *Phys. Rev. Lett.*, 2023, **131**, 238302.
209 C. Chen, S. Liu, X. Q. Shi, H. Chaté and Y. Wu, *Nature*, 2017, **542**, 210–214.
210 M. Riedl, I. Mayer, J. Merrin, M. Sixt and B. Hof, *Nat. Commun.*, 2023, **14**, 5633.
211 M. Bär, R. Großmann, S. Heidenreich and F. Peruani, *Annu. Rev. Condens. Matter Phys.*, 2020, **11**, 441–466.

212 R. Keane and J. Berleman, *Microbiology*, 2016, **162**, 1–11.
213 M. Galbis-Martínez, S. Padmanabhan, F. J. Murillo and M. Elías-Arnanz, *J. Bacteriol.*, 2012, **194**, 1427–1436.
214 A. Holmes, S. Kalvala and D. Whitworth, *Commun. Syst. Inf. World Network*, 2009, **6**, 65–70.
215 K. Subedi and D. Wall, *Front. Microbiol.*, 2022, **13**, 879090.
216 K. J. Dye and Z. Yang, *Front. Microbiol.*, 2022, **13**, 894562.
217 Y. Chen, E. J. Topo, B. Nan and J. Chen, *Front. Microbiol.*, 2024, **14**, 1294631.
218 R. Y. Stanier, *J. Bacteriol.*, 1942, **44**, 405–412.
219 M. J. Kim and K. S. Breuer, *Phys. Fluids*, 2004, **16**, L78–L81.
220 A. Jepson, V. A. Martinez, J. Schwarz-Linek, A. Morozov and W. C. K. Poon, *Phys. Rev. E: Stat., Nonlinear, Soft Matter Phys.*, 2013, **88**, 041002.
221 A. Morozov and D. Marenduzzo, *Soft Matter*, 2014, **10**, 2748.
222 X.-L. Wu and A. Libchaber, *Phys. Rev. Lett.*, 2000, **84**, 3017–3020.
223 G. L. Miño, J. Dunstan, A. Rousselet, E. Clément and R. Soto, *J. Fluid Mech.*, 2013, **729**, 423–444.
224 W. Sempels, R. D. Dier, H. Mizuno, J. Hofkens and J. Vermant, *Nat. Commun.*, 2013, **4**, 1757.
225 D. Yanni, A. Kalziqi, J. Thomas, S. L. Ng, S. Vivek, W. C. Ratcliff, B. K. Hammer and P. J. Yunker, *arXiv*, 2017, preprint, arXiv:1707.03472, DOI: **10.48550/arXiv:1707.03472**.
226 T. Andac, P. Weigmann, S. K. P. Velu, E. Pinçe, G. Volpe, G. Volpe and A. Callegari, *Soft Matter*, 2019, **15**, 1488–1496.
227 J. A. A. D. Angel, A. E. Escalante, L. P. Martínez-Castilla and M. Benítez, *Dev., Growth Differ.*, 2018, **60**, 121–129.
228 Z. Zhang, O. A. Igoshin, C. R. Cotter and L. J. Shimkets, *Biophys. J.*, 2018, **115**, 2499–2511.
229 W. Zhang, Y. Wang, H. Lu, Q. Liu, C. Wang, W. Hu and K. Zhao, *Appl. Environ. Microbiol.*, 2020, 86.
230 R. Balagam, P. Cao, G. P. Sah, Z. Zhang, K. Subedi, D. Wall and O. A. Igoshin, *mSystems*, 2021, **6**(6), e00720-21.
231 J. Starruß, T. Bley, L. Søgaard-Andersen and A. Deutsch, *J. Stat. Phys.*, 2007, **128**, 269–286.
232 A. B. Holmes, S. Kalvala and D. E. Whitworth, *PLoS Comput. Biol.*, 2010, **6**, e1000686.
233 R. Balagam and O. A. Igoshin, *PLoS Comput. Biol.*, 2015, **11**, e1004474.